

# one-dimensional quantum graphene devices

Herre van der Zant



vanderZant lab

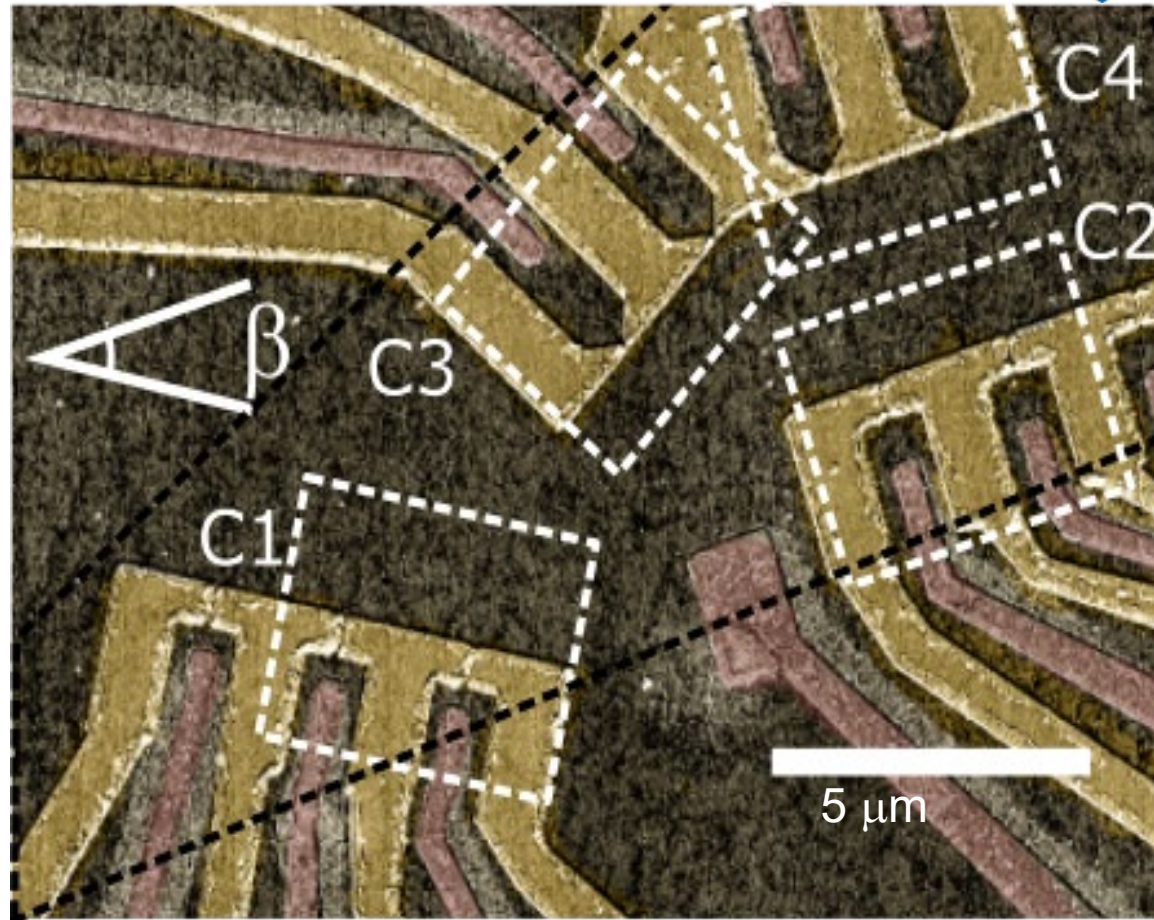
<https://vanderzantlab.tudelft.nl/>

## quantum electronics:

- single molecules
- bionanowires
- graphene nanoribbons
- (spin transition) nanoparticles
- 2D materials

## nanomechanics:

- 2D magnetic materials
- CDW systems
- Ferroelectrics



GRAPHENE FLAGSHIP



MARIE SKŁODOWSKA-CURIE ACTIONS

Research Fellowship Programme



#EU\_eic

European  
eic **INNOVATION**  
Council

# What is a quantum device?

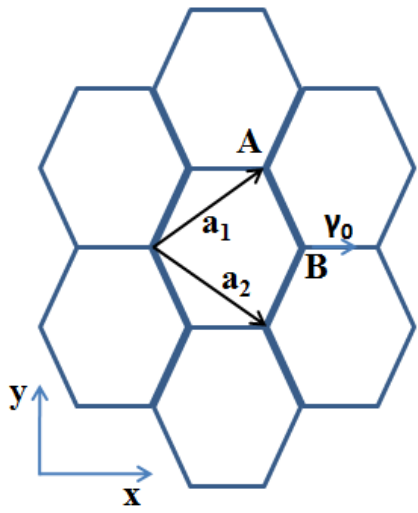
(and what would one need to make them?)

# What is a quantum device?

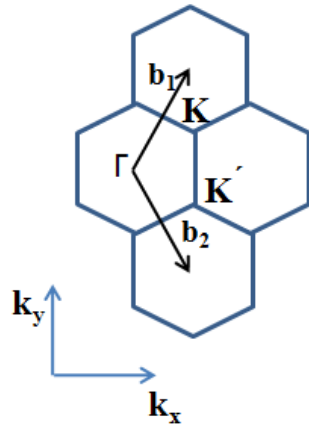
Two levels of quantum-ness:

- 1) Devices that operate using discrete levels or through interference effects involving the electron's phase of the wave function (quantum wires, quantum point contacts, charge sensors, THz (radiation) sensors, Quantum Hall standard, ....)
- 2) Devices that use a coherent superposition state (quantum coherence, sensors at the quantum limit, qubits, quantum encryption and information processing, ...)

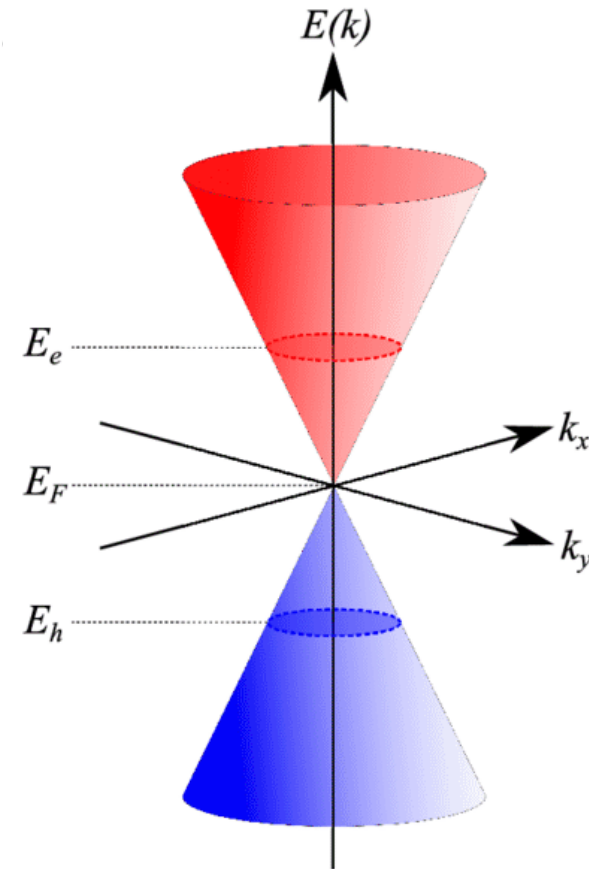
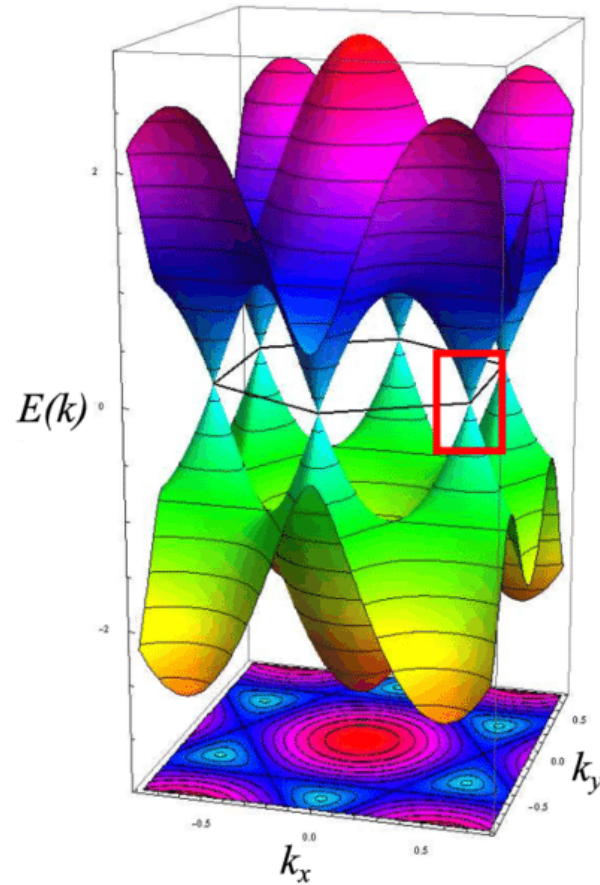
# graphene band structure: two Dirac cones, two valleys, K and K' (or sometimes denoted as -K)



real space



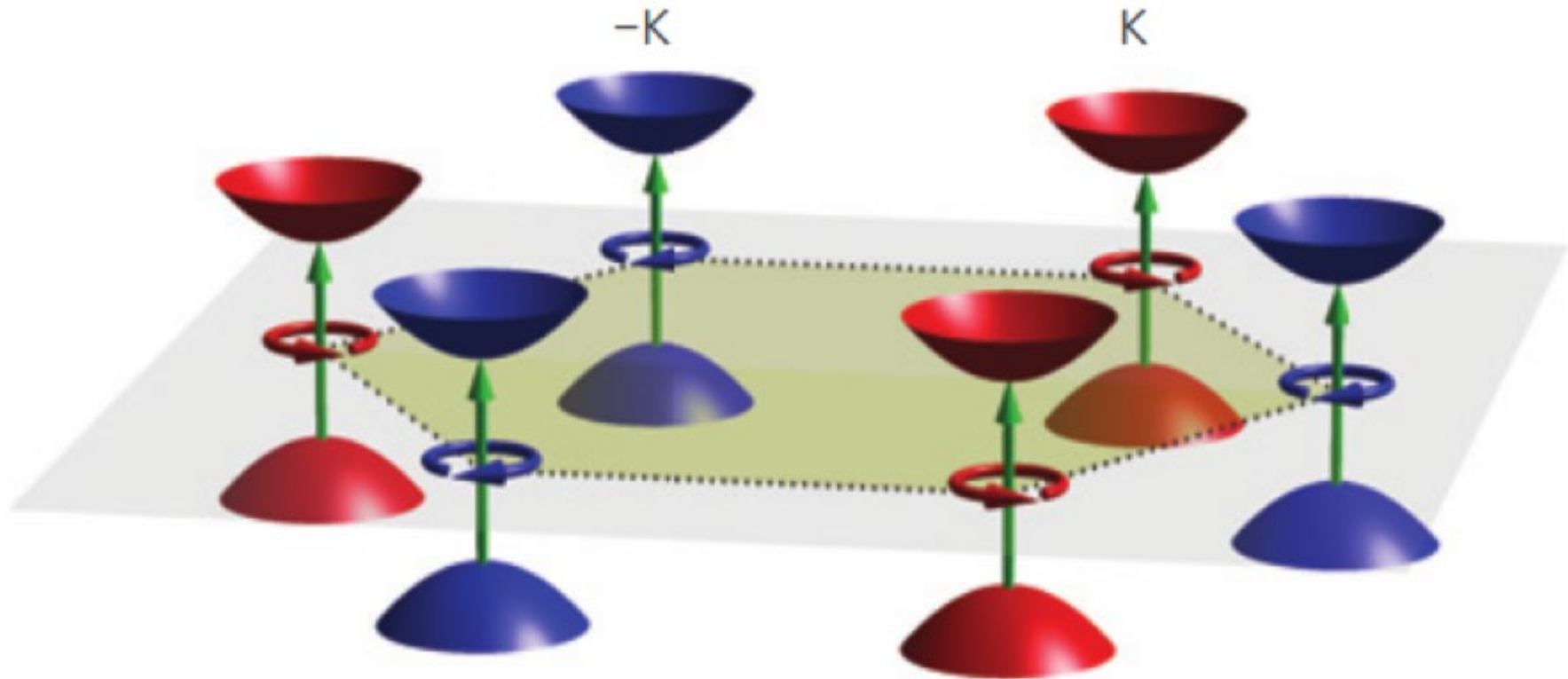
reciprocal space



# 2D material quantum devices

## electronics, spintronics, valleytronics

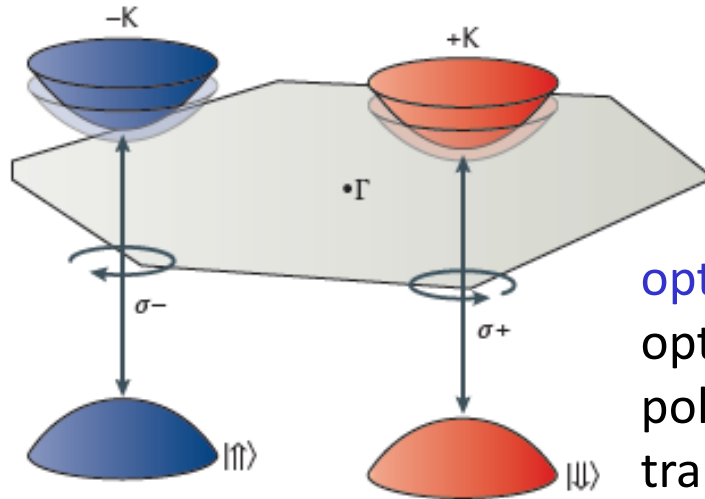
- electronics: electrons as information carriers
- spintronics: electron spin as information carrier
- valleytronics: valley-dependent carrier transport and optoelectronic response



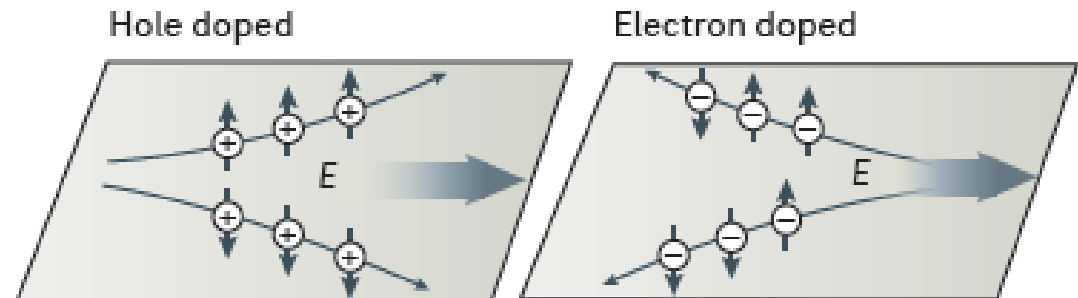
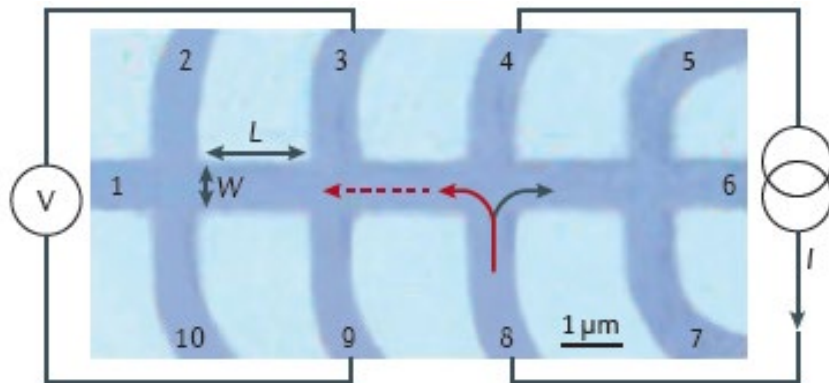
Valleys can be represented by a binary pseudospin behaving like a spin-1/2 system; electrons in the  $+K$  valley can be labelled as valley-pseudospin up and electrons in the  $-K$  with valley-pseudospin down. Carrier polarization in one of the valleys can thus store binary information.

## Valleytronics in 2D materials

John R. Schaibley<sup>1</sup>, Hongyi Yu<sup>2</sup>, Genevieve Clark<sup>3</sup>, Pasqual Rivera<sup>1</sup>, Jason S. Ross<sup>3</sup>, Kyle L. Seyler<sup>1</sup>, Wang Yao<sup>2</sup> and Xiaodong Xu<sup>1,3</sup>



**optoelectronics:** valley dependent optical selection rules, e.g. left circular polarized light couples to interband transitions in the  $-K$  valley



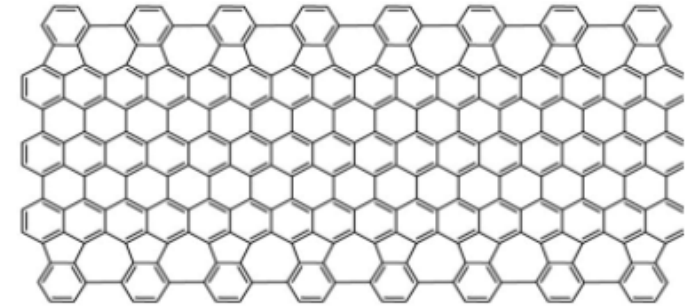
valley Hall effect with opposite Berry curvature (acts as an effective magnetic field) for the different valleys in presence of **broken inversion symmetry**

# 1D graphene quantum devices

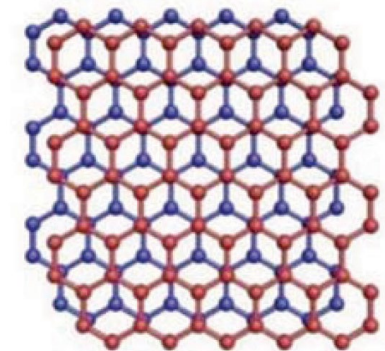
## different approaches, different platforms

- **graphene nanoribbons**: bottom-up defined atomically precise

ac-zigzag  
APR

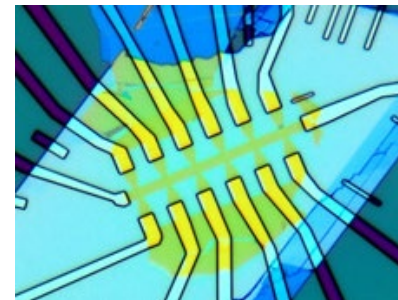


- **bi-layer graphene** (not twisted): band gap and electrostatically defined device geometries



AB-stacked  
bilayer-graphene

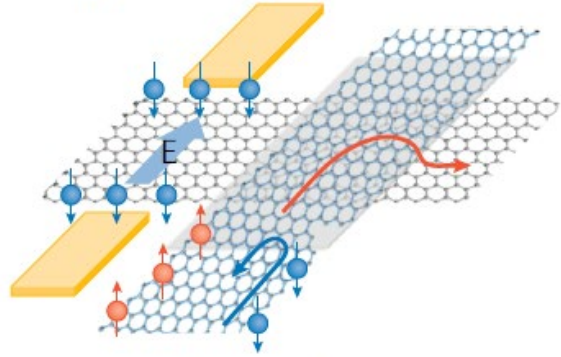
- quantum Hall states in **heterostructures** with graphene to introduce broken inversion symmetry



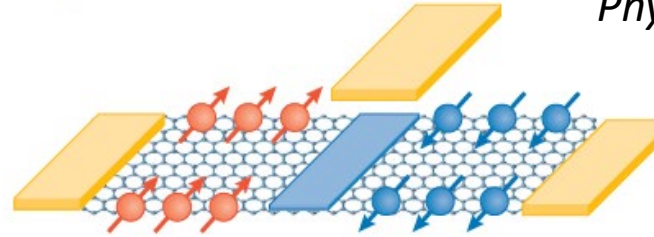
# graphene nanoribbons for quantum electronics and spintronics

*H. Wang et al., Nature Reviews Physics 3 (2021) 791–802*

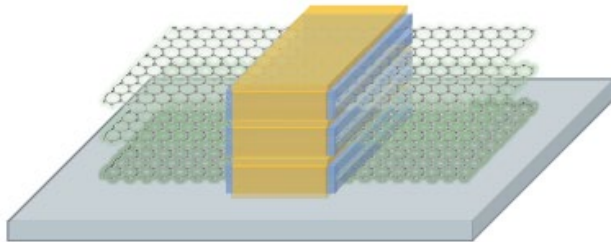
**a** Magnetic tunnel junction



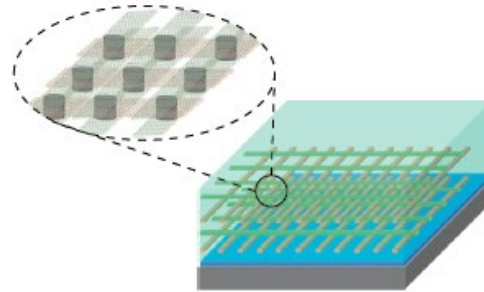
**b** Spin FET



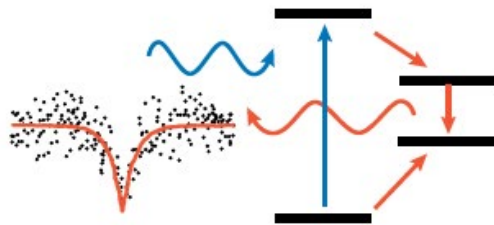
**c** 3D gate-all-around FET



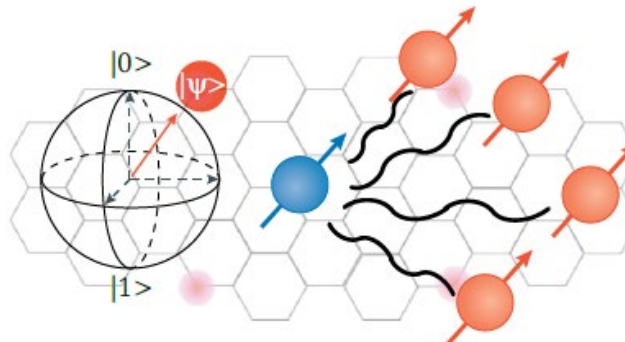
**d** 3D heterogeneous integration



**e** Single-photon emitters



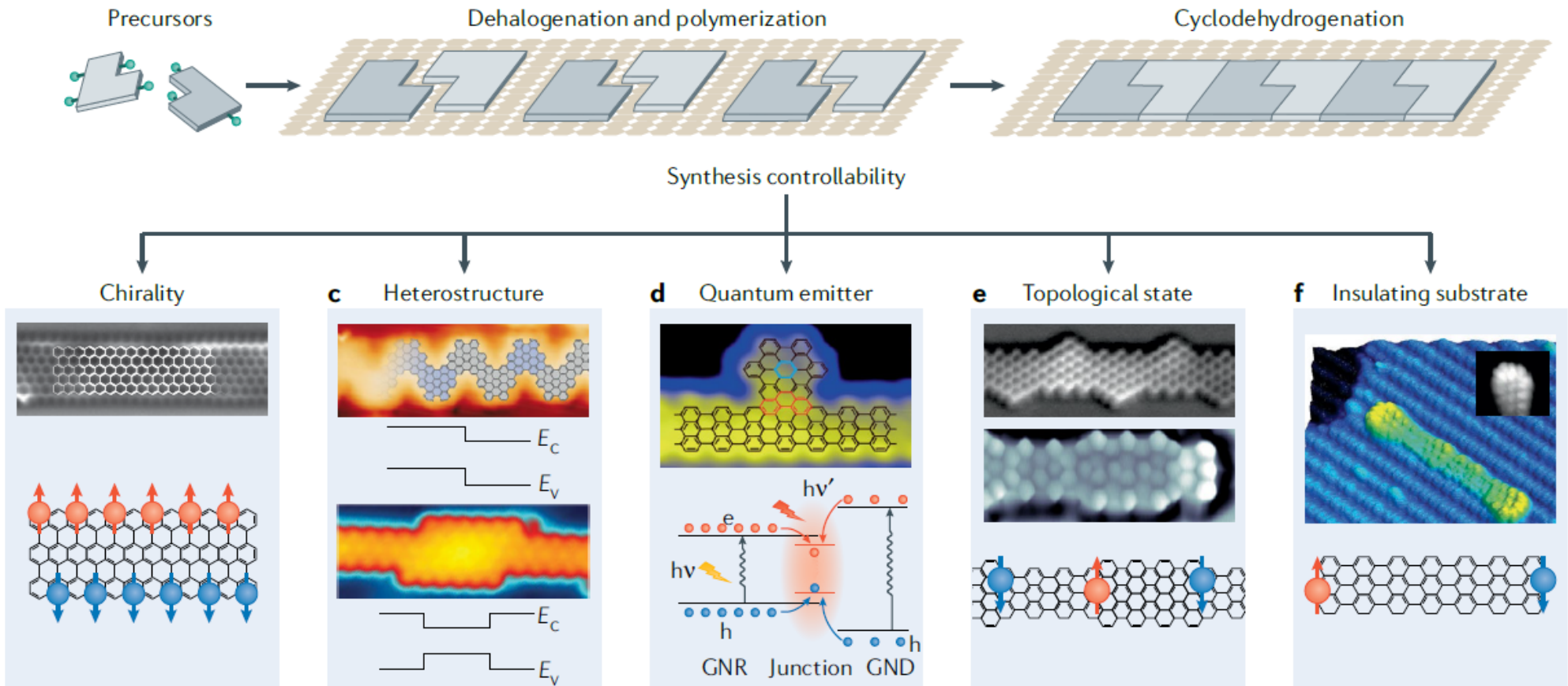
**f** Quantum computing and simulation



# bottom-up atomically precise graphene nanoribbons

H. Wang et al., *Nature Reviews Physics* **3** (2021) 791–802

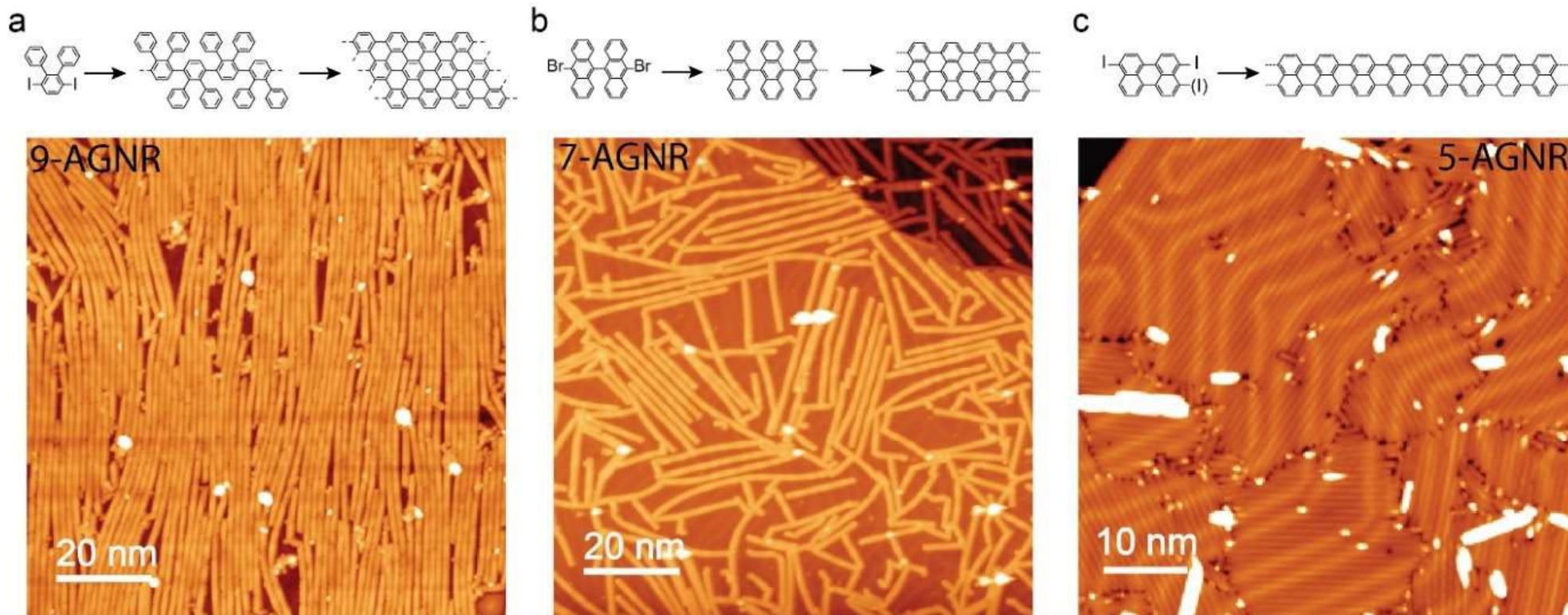
to avoid irregular edges introduced in top-down etched devices



grown in ultra-high vacuum on gold surfaces but for a device one has to (i) **transfer** the nanoribbons from the substrates made in vacuum and (ii) make **contacts** to them

# non-functionalized graphene nanoribbons

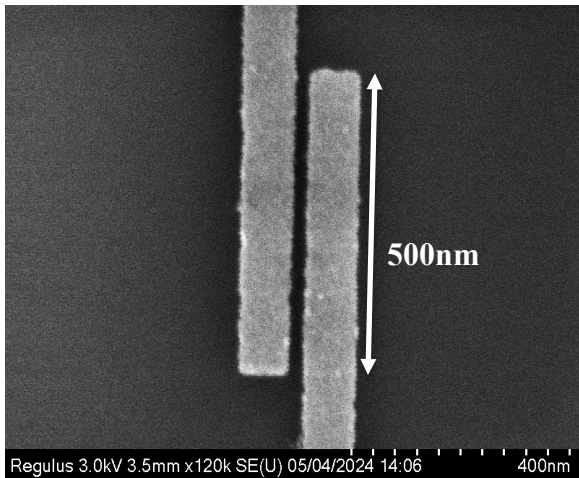
Armchair GNRs can be divided into three families, depending on whether their width is:  $3p$  (medium bandgap),  $3p + 1$  (large bandgap) or  $3p+2$  (small bandgap) where  $p$  is an integer. Within each family, the bandgap increases monotonically as the width decreases.



**our target: 9-atom wide graphene nanoribbon (armchair): lengths (up to 40 -50 nm) and relatively stable; bandgap: 1.4 eV**

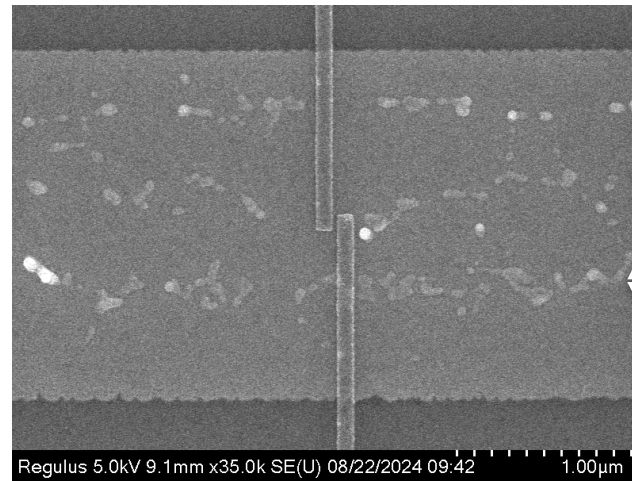
# pre-patterned electrodes

different contact and gate geometries and different metals (Pt, MoRe, Pd)



**global back gate**

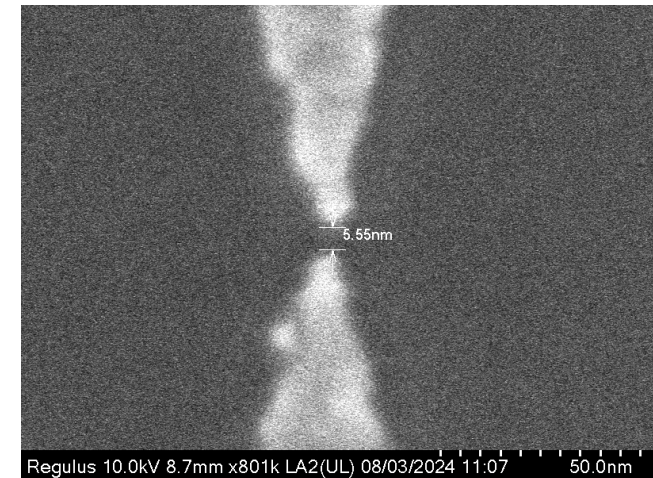
**large overlap to contact  
several APRs in parallel**



**local back gate**

**large overlap to contact  
several APRs in parallel**

**as we found that the  
global gate can be very  
inefficient**

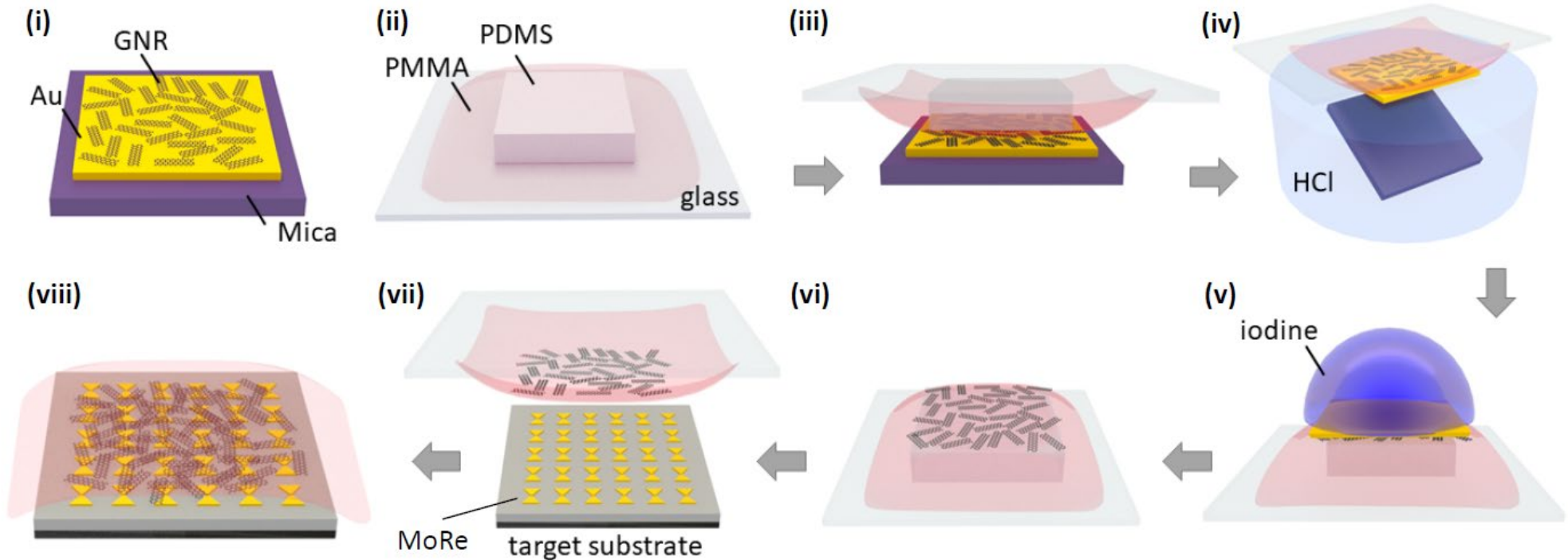


**global/local back gate**

**small overlap to contact a  
single APR**

# transferring atomically precise graphene nanoribbons

a PMMA-membrane transfer method was developed that avoids contact of the target substrate with liquids; GNRs can then be deposited in an aligned manner using a dry transfer stage

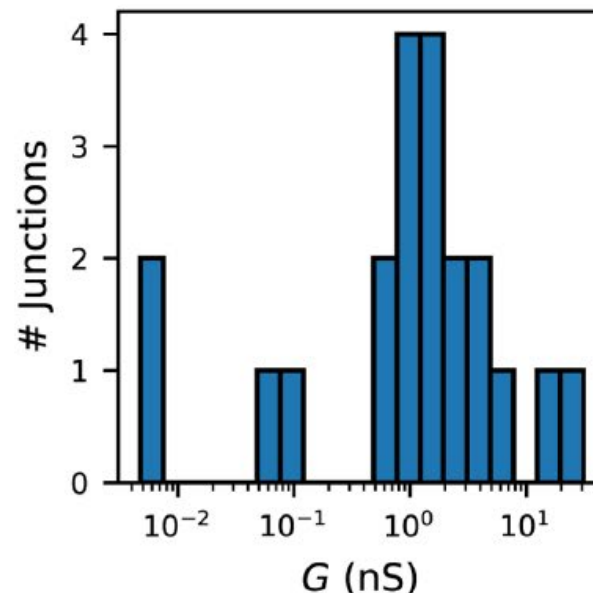
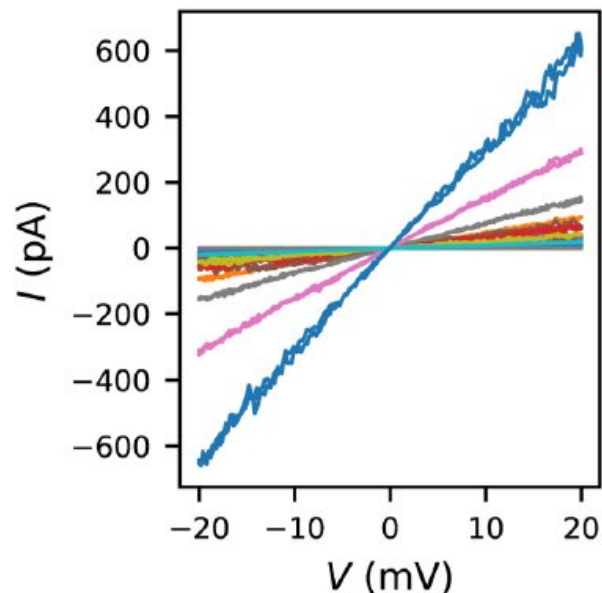
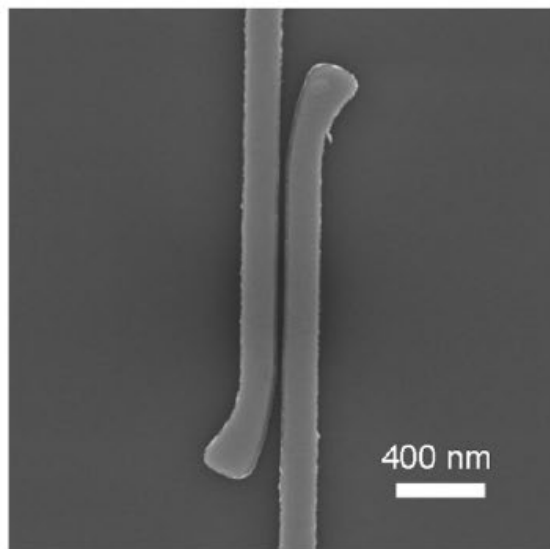


## MoRe Electrodes with 10 nm Nanogaps for Electrical Contact to Atomically Precise Graphene Nanoribbons

Damian Bouwmeester,\* Talieh S. Ghiasi, Gabriela Borin Barin, Klaus Müllen, Pascal Ruffieux, Roman Fasel, and Herre S. J. van der Zant

# bottom contacting graphene nanoribbons

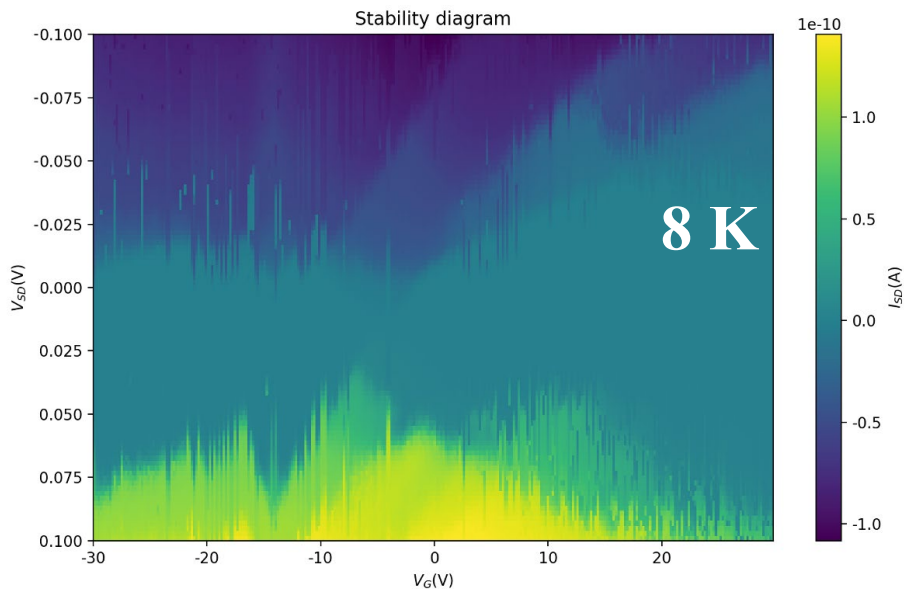
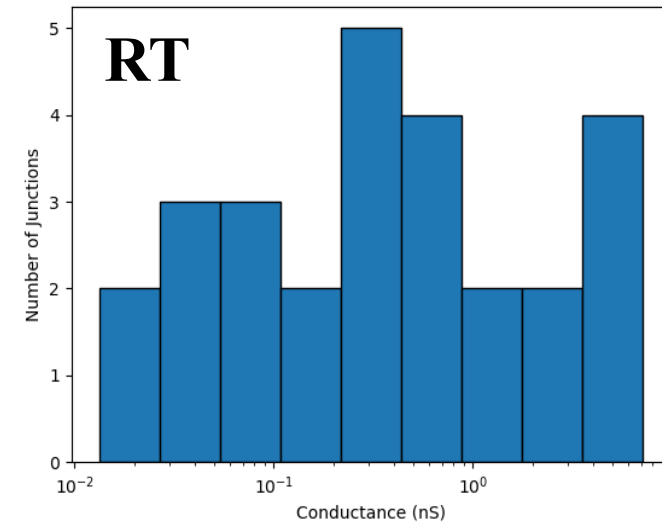
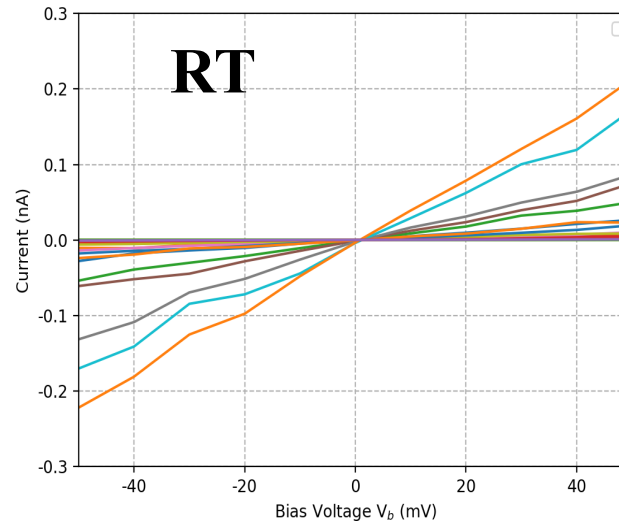
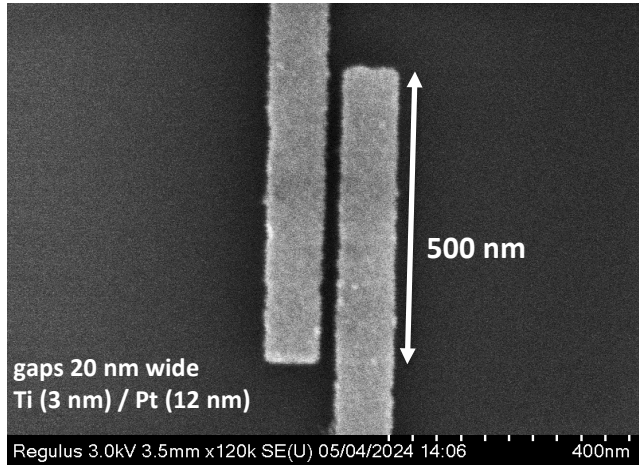
use same strategy as for contacting carbon nanotubes (MoRe and Pd as electrodes)



## MoRe Electrodes with 10 nm Nanogaps for Electrical Contact to Atomically Precise Graphene Nanoribbons

Damian Bouwmeester,\* Talieh S. Ghiasi, Gabriela Borin Barin, Klaus Müllen, Pascal Ruffieux, Roman Fasel, and Herre S. J. van der Zant

# Pt bottom contacting graphene nanoribbons

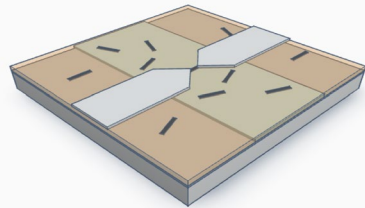
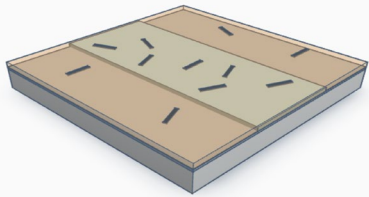
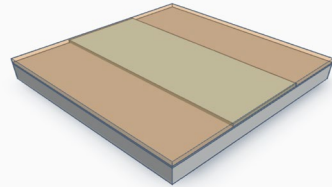
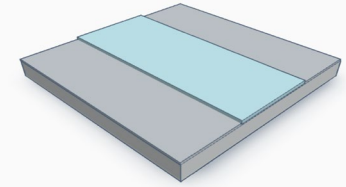


- successfully captured 9AGNRs by using pre-patterned electrodes
- IV measurements can be performed at room and low temperatures
- the long gaps capture multiple GNRs in between, leading to multi-dot behaviour (with GNRs in series) in the stability diagram at low temperatures

# top contacts with sub-10 nm spacing

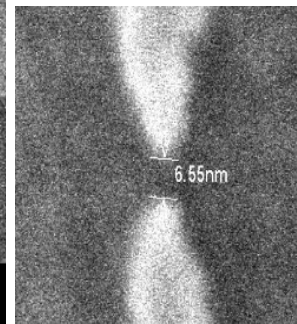
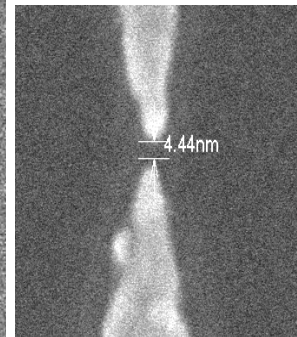
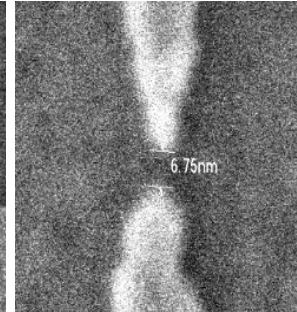
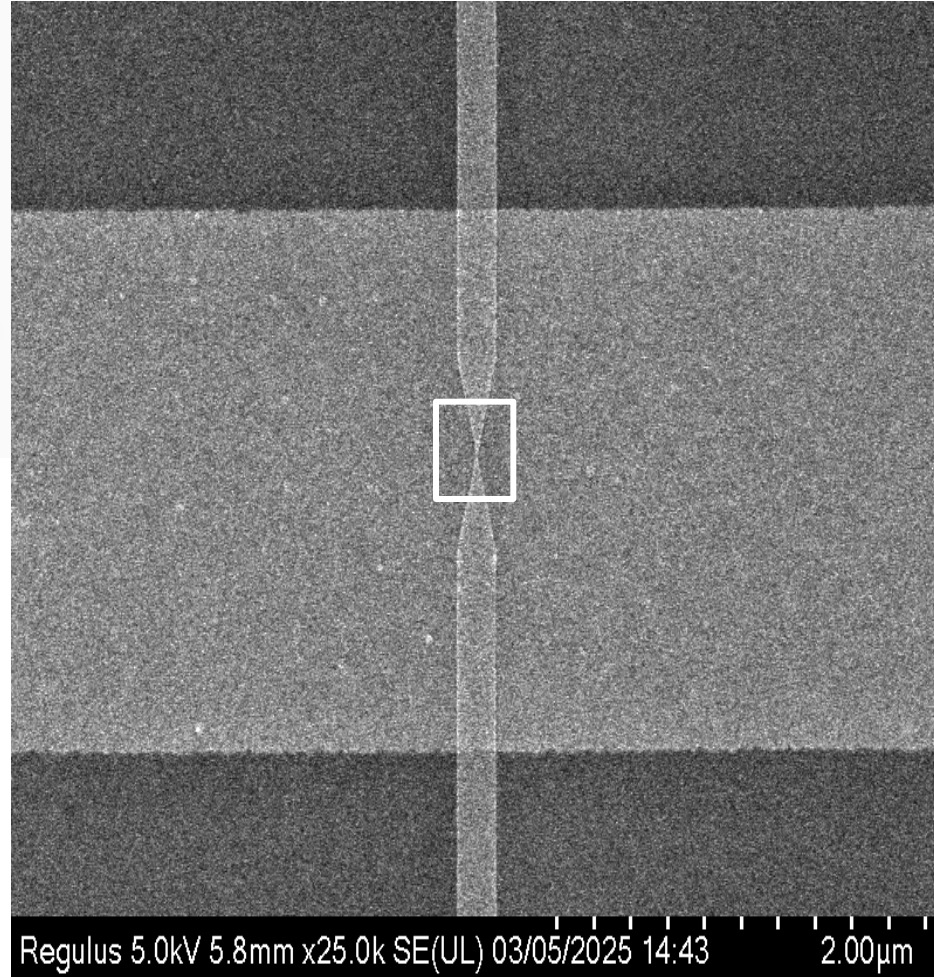
local back gate: 1 nm Ti and 7 nm Pd

7 nm ALD grown  $\text{HfO}_2$



9-AGNRs are transferred

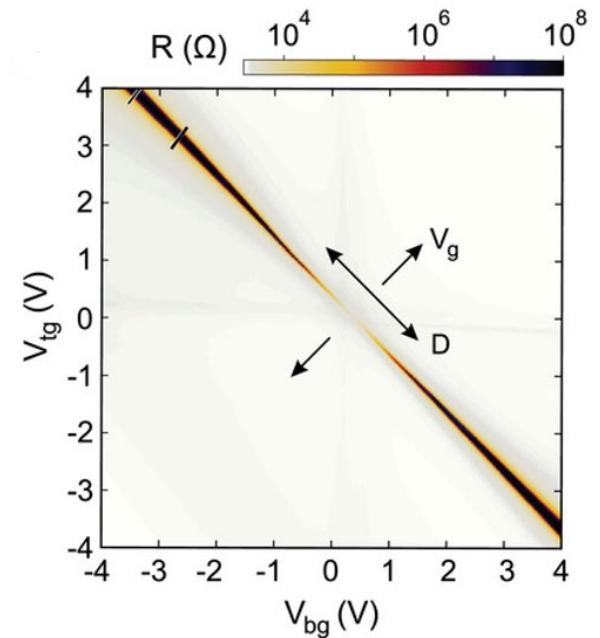
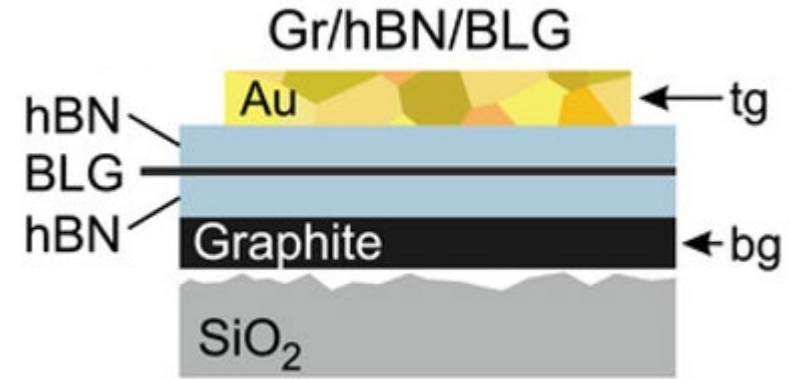
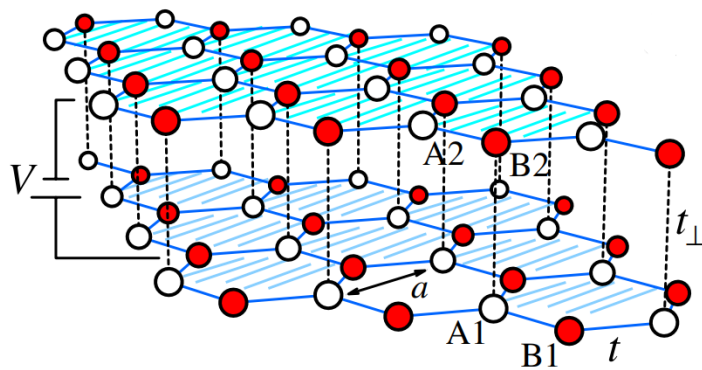
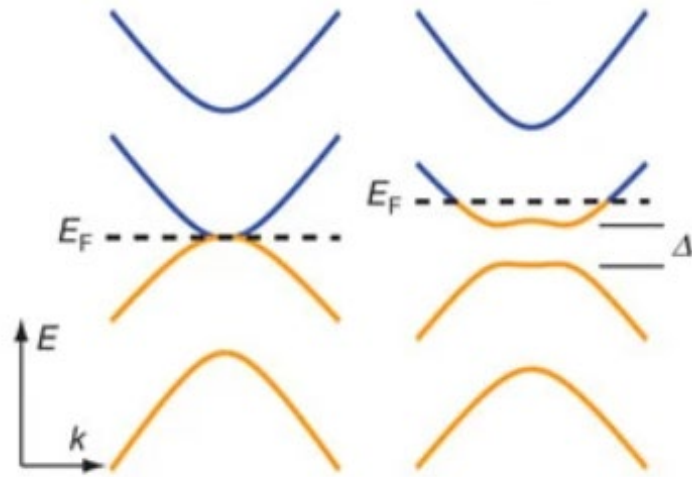
needle-like 12 nm Pd electrodes are then patterned on top



# **bi-layer graphene quantum devices**





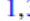





# bi-layer graphene quantum devices

inversion symmetry broken by an electric applied across the two layers: band gap opens up

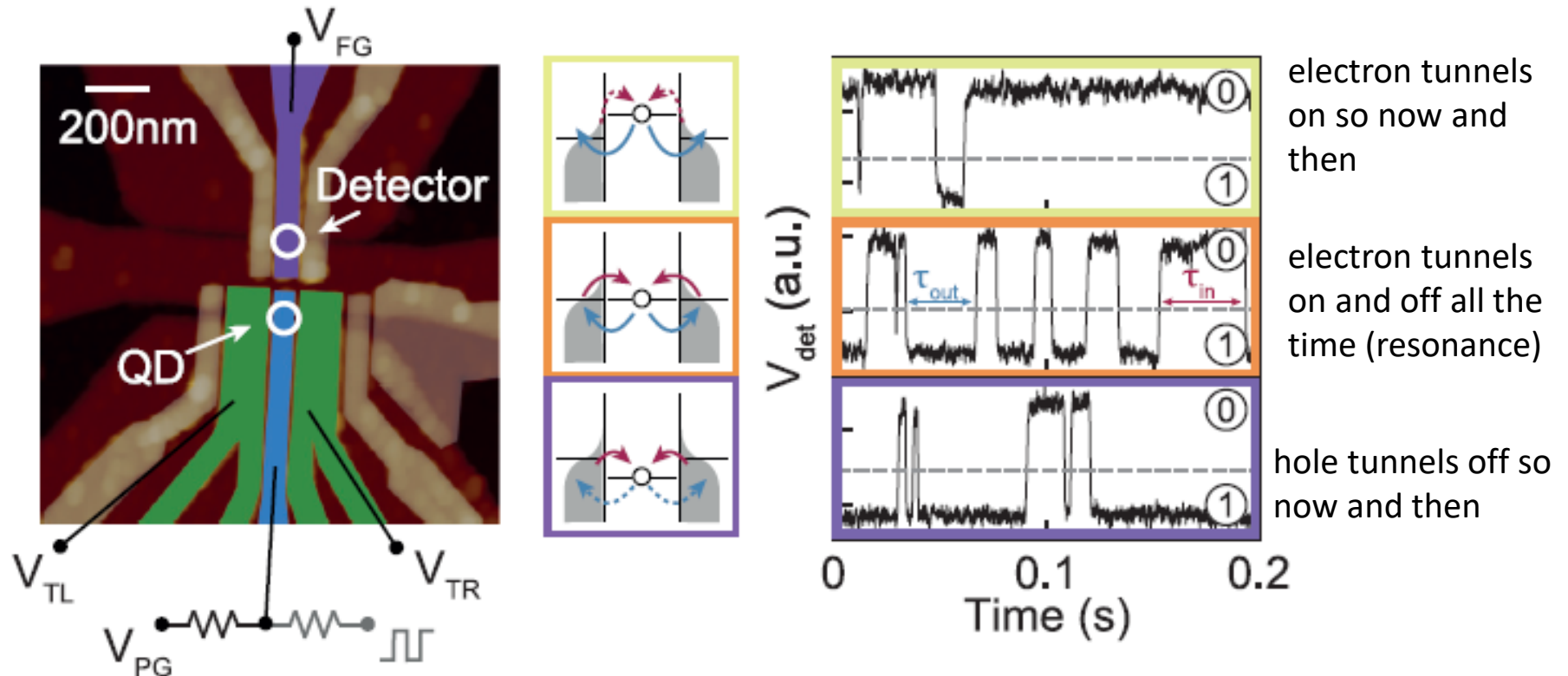


Icking et al., *Adv. Elec. Mater.* **8** (2022) 2200510  
 Zhang et al., *Nature* **459** (2009) 820

## Counting statistics of single electron transport in bilayer graphene quantum dots

Rebekka Garreis <sup>1,\*</sup> Jonas Daniel Gerber <sup>1</sup> Veronika Stará <sup>2</sup> Chuyao Tong <sup>1</sup> Carolin Gold <sup>1,3</sup> Marc Rössli <sup>1</sup>  
Kenji Watanabe <sup>4</sup> Takashi Taniguchi <sup>4</sup> Klaus Ensslin <sup>1</sup> Thomas Ihn <sup>1</sup> and Annika Kurzmann <sup>1,5</sup>

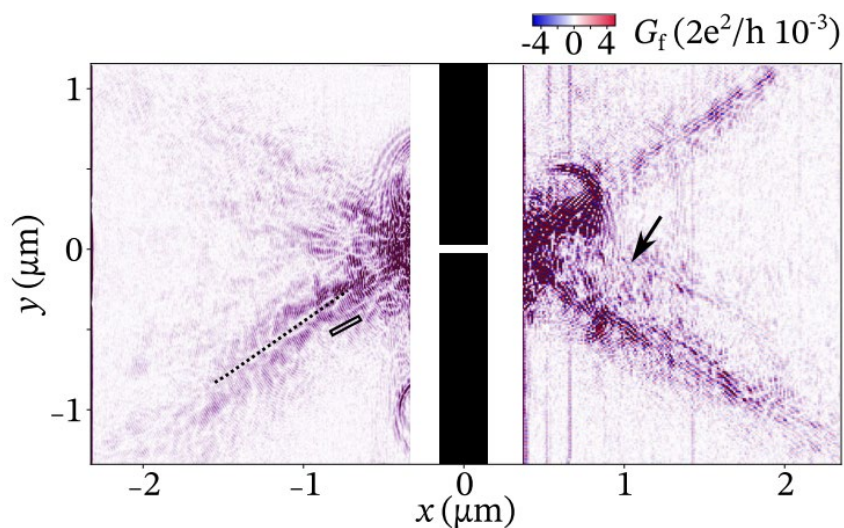
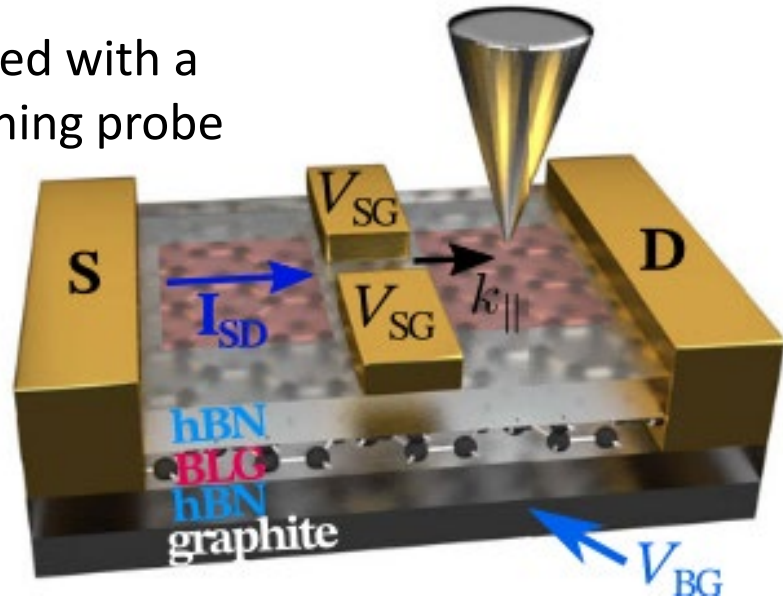
two capacitively coupled quantum dots: one acts as the detector of the charge in the other



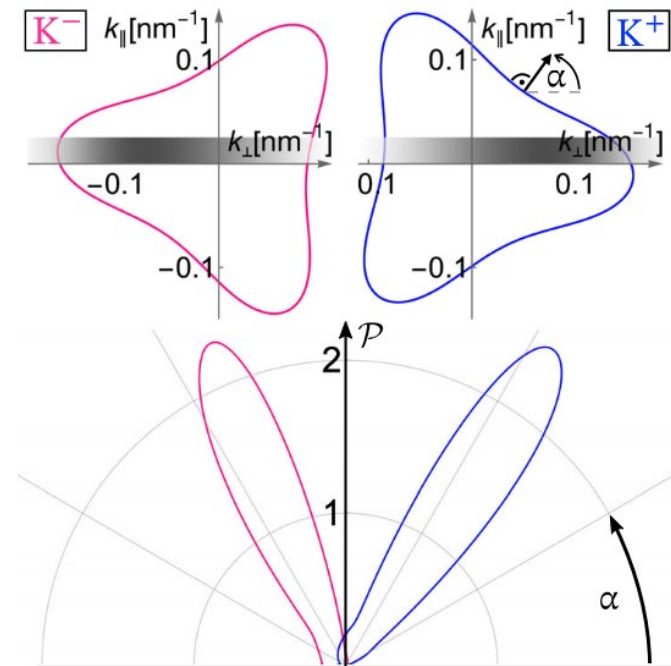
high-quality devices with a high degree of control

# valley polarized electron jets due to triangular warping in bilayer graphene (BLG)

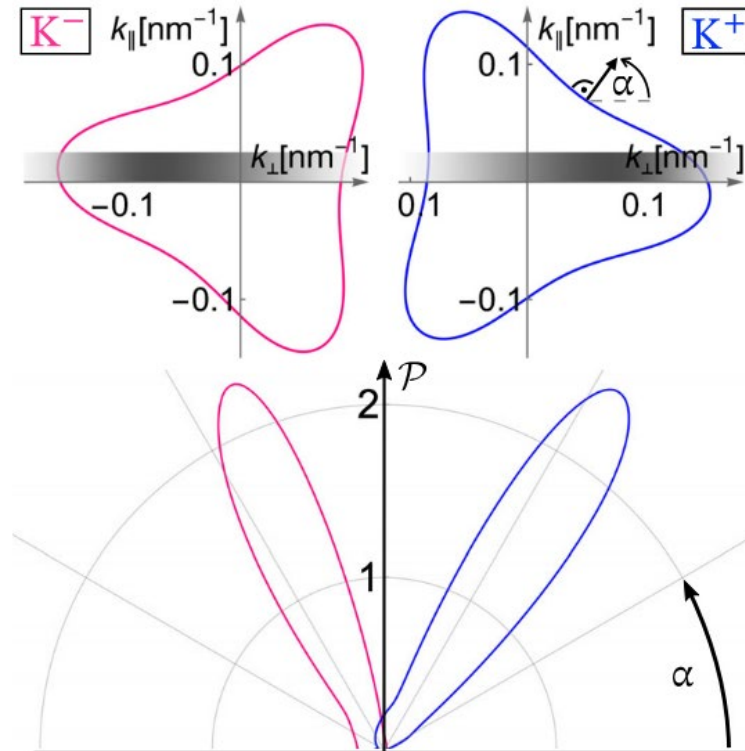
imaged with a scanning probe



the Fermi surfaces are not spherical in BLG and is different (rotated) for the two valleys

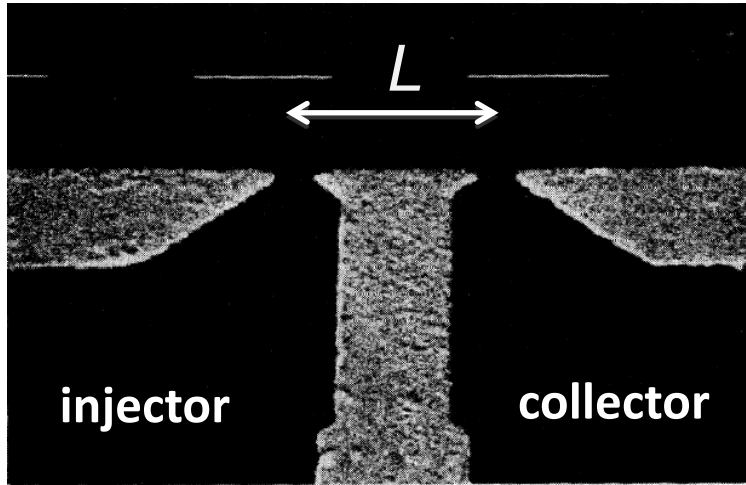


# How to control valley-polarized currents in a device?



using **electron jets** steered by a magnetic field in **transverse electron focussing** with **quantum point contacts** as injectors and collectors

# classical ballistic transport: transverse electron focusing



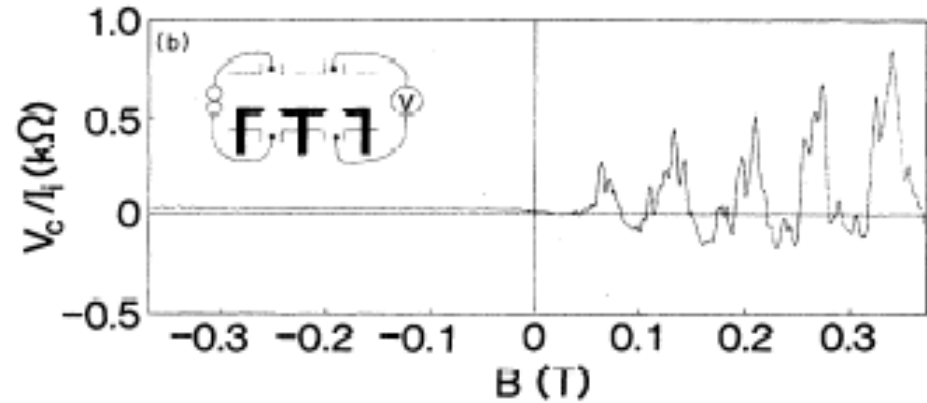
top-gate structure  
2DEG (GaAs-Al<sub>x</sub>Ga<sub>1-x</sub>As)

$$n = 3.5 \cdot 10^{15} \text{ m}^{-2}$$

$$\mu = 90 \text{ m}^2/\text{Vs}$$

$$L = 3 \text{ } \mu\text{m}$$

$\ell_e = 9 \text{ } \mu\text{m}$  (mean free path, no scattering within this length scale)



use perpendicular magnetic field to focus electron jets leading to peaks in the non-local voltage



cyclotron radius:  $r_c = mv_F/eB$

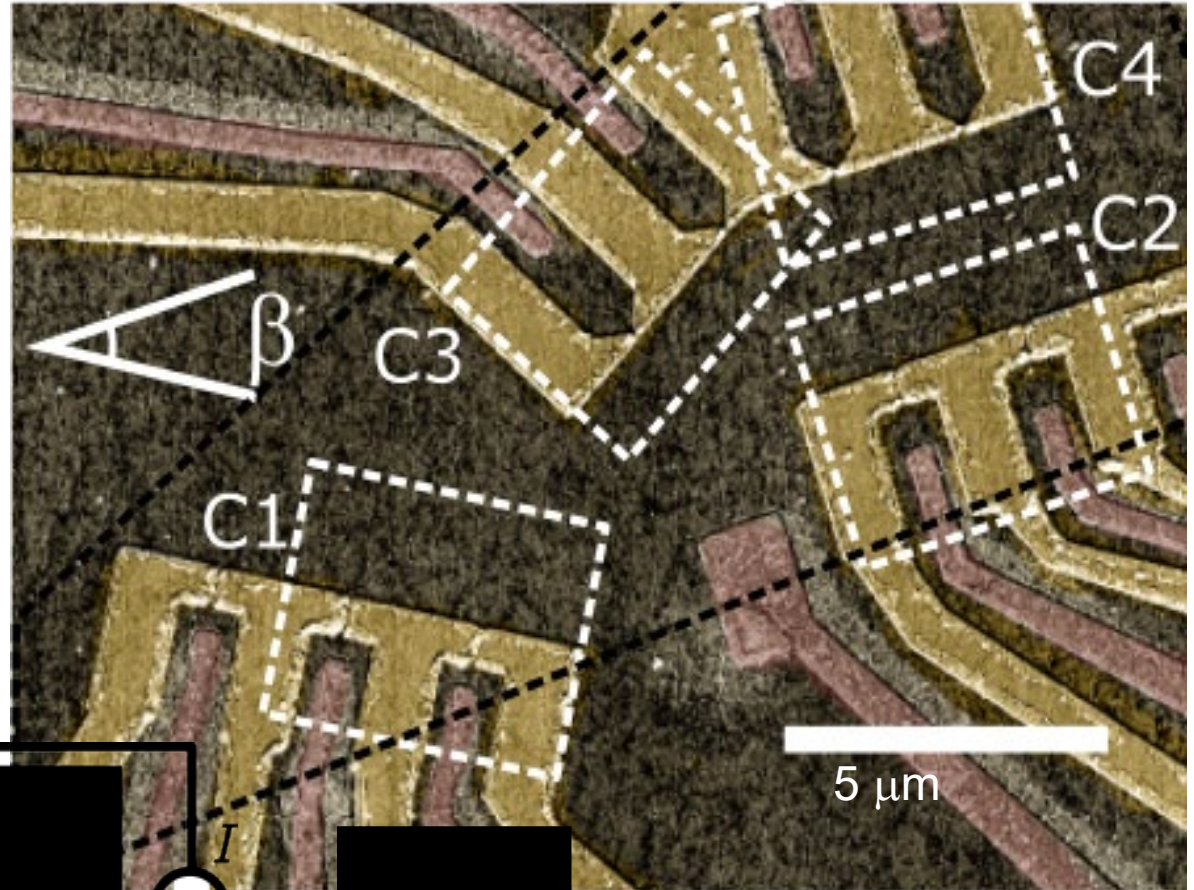
$$B_p = p^*(2mv_F/eL)$$

( $p - 1$ ) = number of reflections

# our BLG device

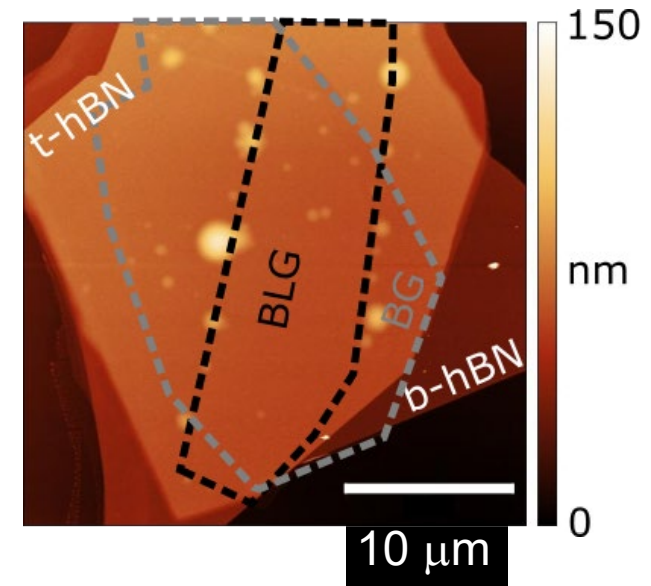
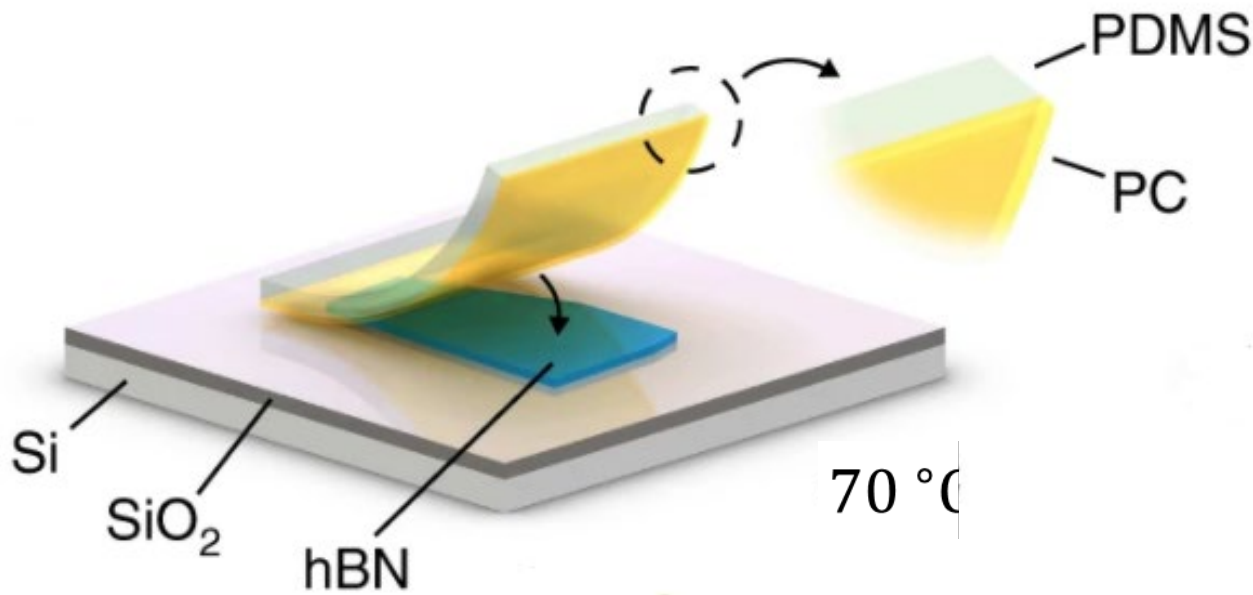


Josep Ingla-Aynés



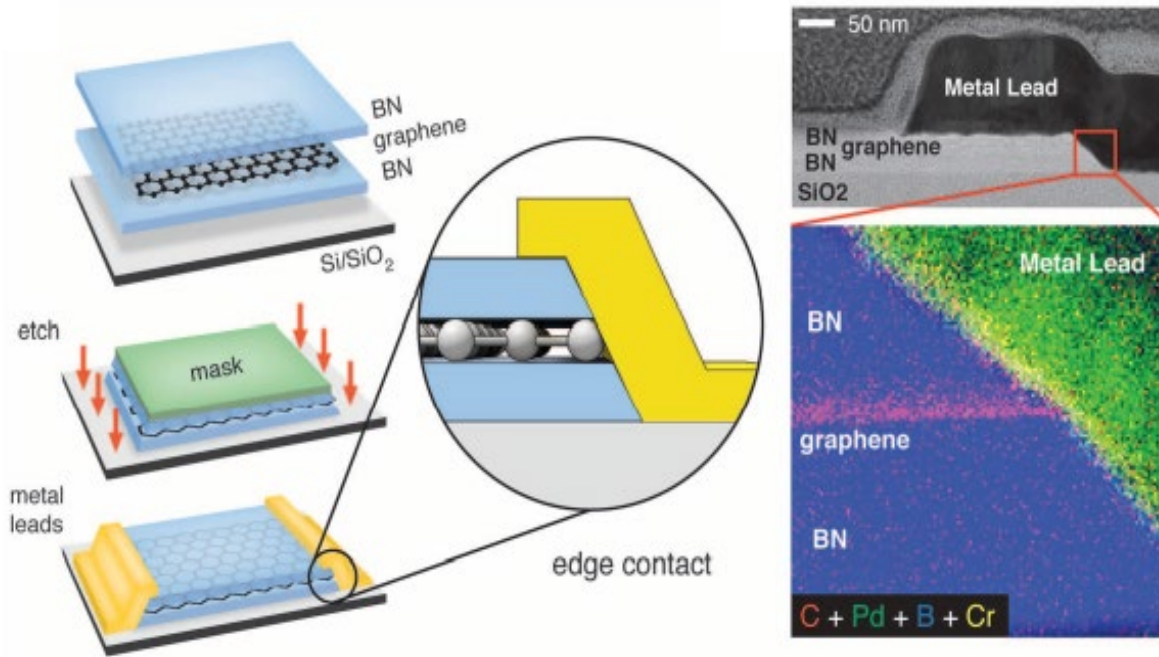
*J. Ingla-Aynés et al., Nano Lett.*  
**23** (2023) 5453 – 5459

# fabrication: dry transfer technique (4 layered materials)

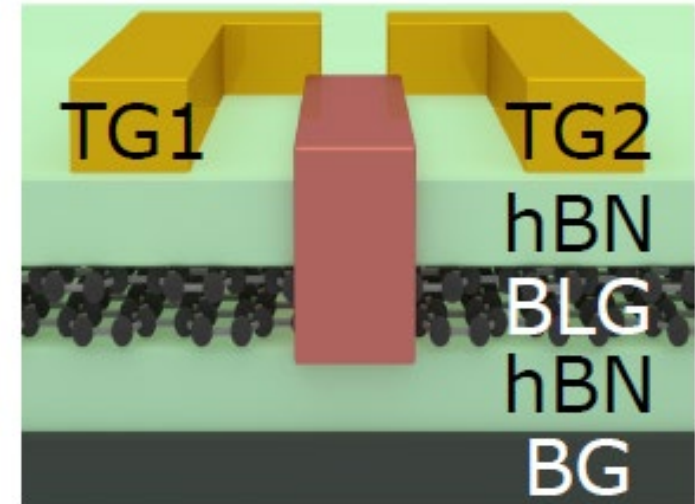


*Purdie et al. Nature Commun.* **9** (2018) 5387 (2018)  
*Zomer et al. Appl. Phys. Lett.* **105** (2014) 013101 (2014)

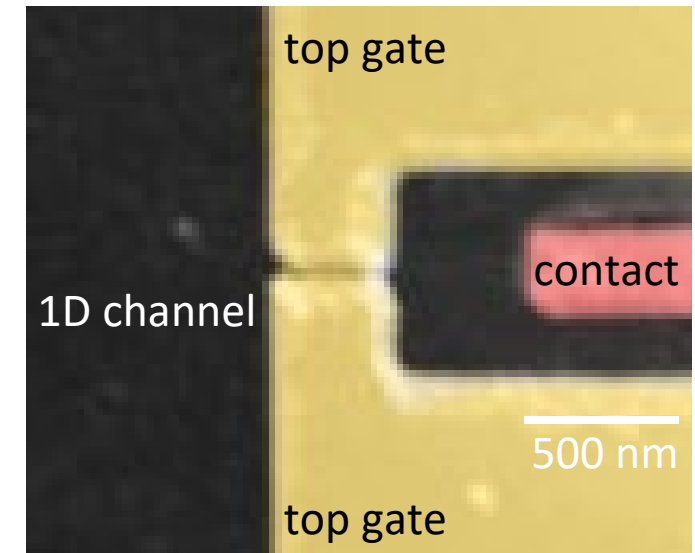
# fabrication: side (edge) contacts to the BLG and metallic top gates



L. Wang et al. *Science* **342** (2013) 614



side view quantum point contact



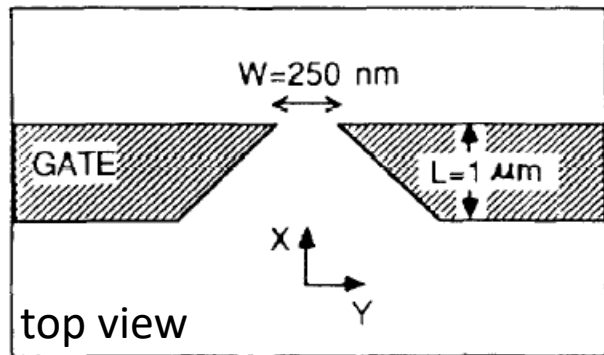
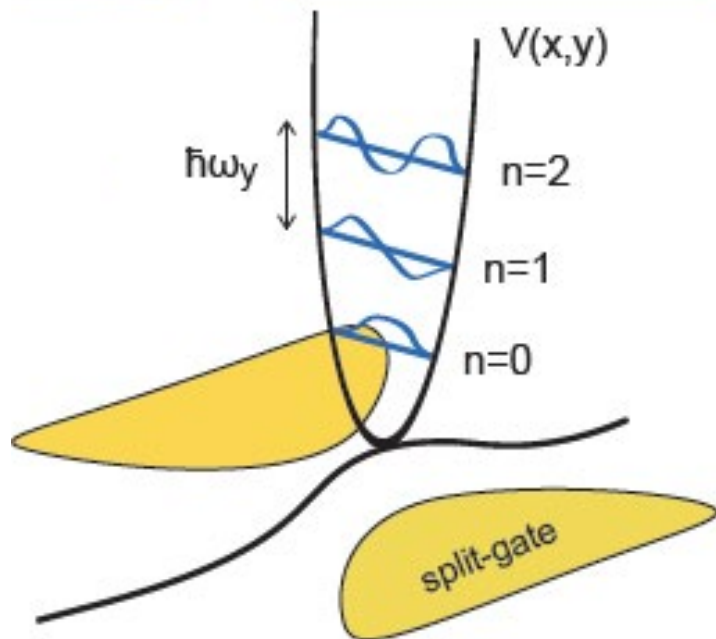
top view quantum point contact

# intermezzo: quantum point contacts and quantized conductance

VOLUME 60, NUMBER 9

PHYSICAL REVIEW LETTERS

29 FEBRUARY 1988



2DEG ( $\text{GaAs-Al}_x\text{Ga}_{1-x}\text{As}$ )

## Quantized Conductance of Point Contacts in a Two-Dimensional Electron Gas

B. J. van Wees

*Department of Applied Physics, Delft University of Technology, 2628 CJ Delft, The Netherlands*

H. van Houten, C. W. J. Beenakker, and J. G. Williamson,  
*Philips Research Laboratories, 5600 JA Eindhoven, The Netherlands*

L. P. Kouwenhoven and D. van der Marel

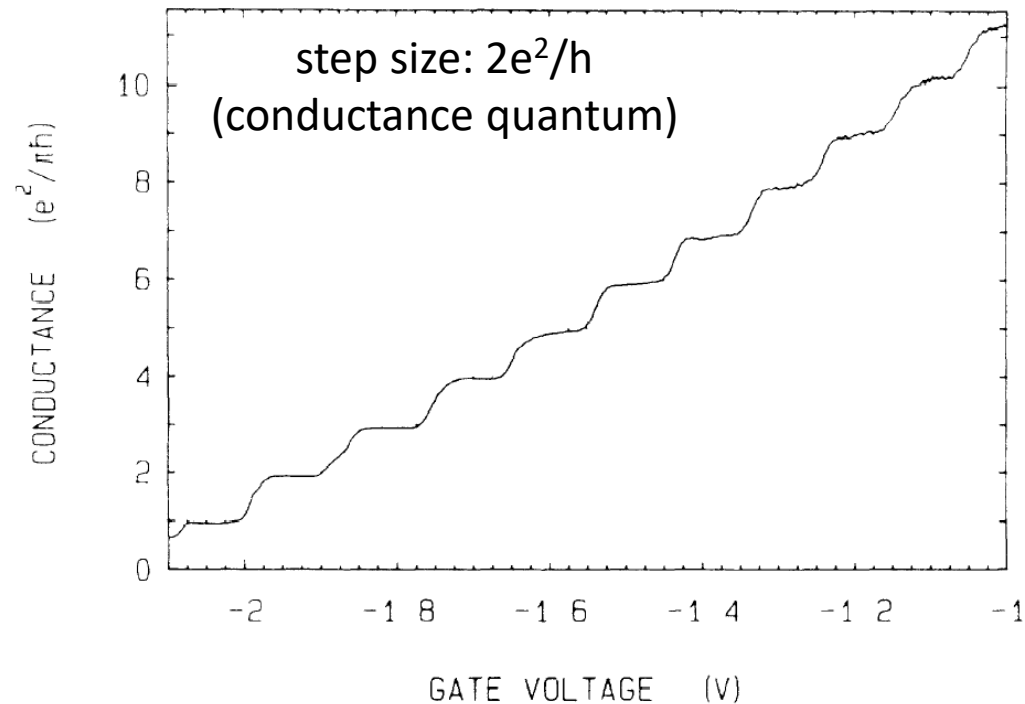
*Department of Applied Physics, Delft University of Technology, 2628 CJ Delft, The Netherlands*

and

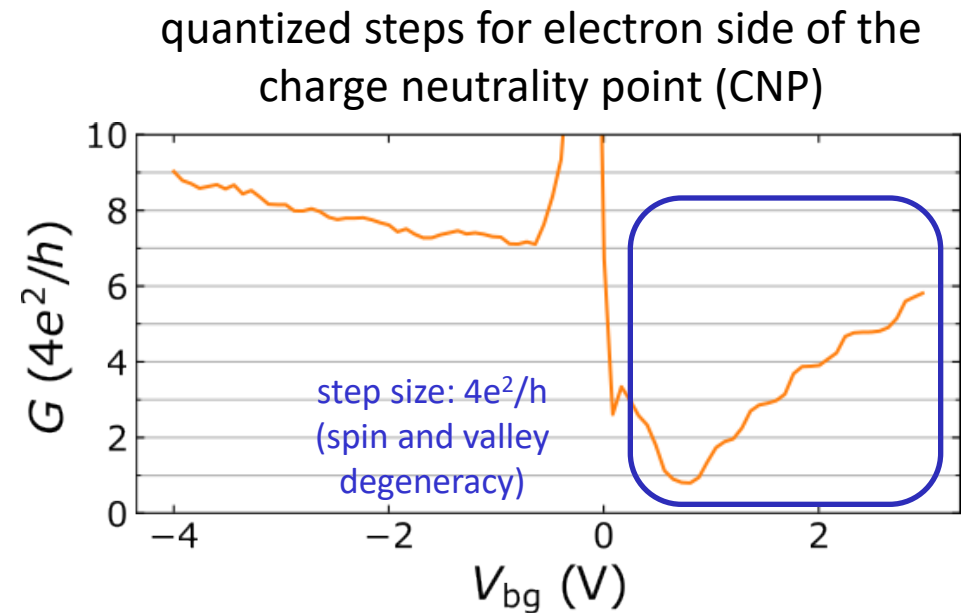
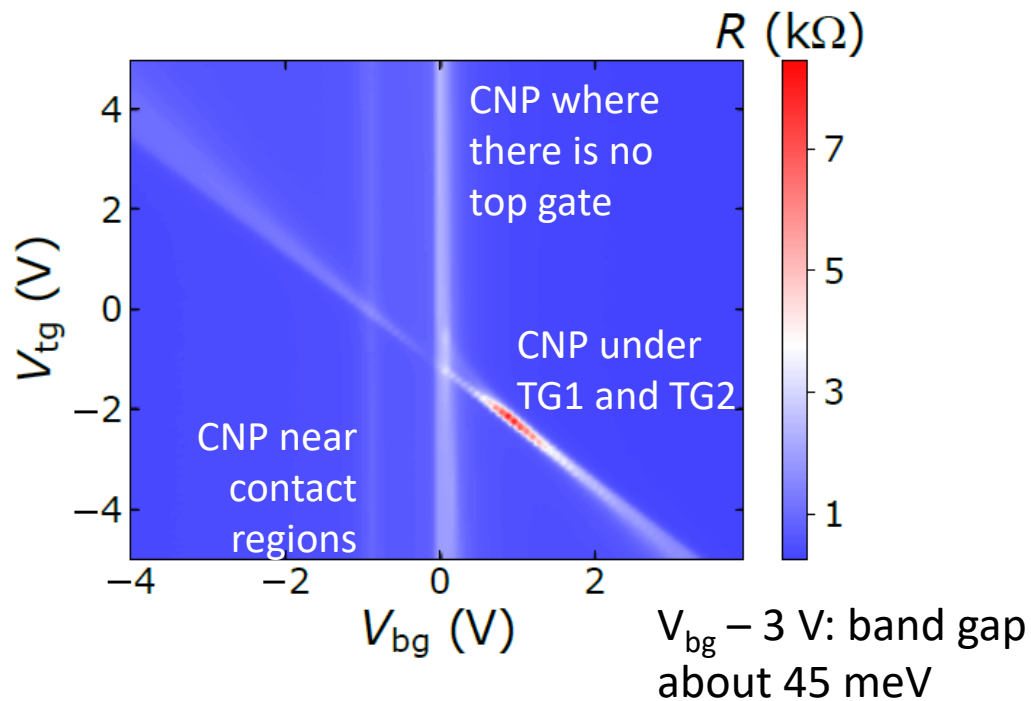
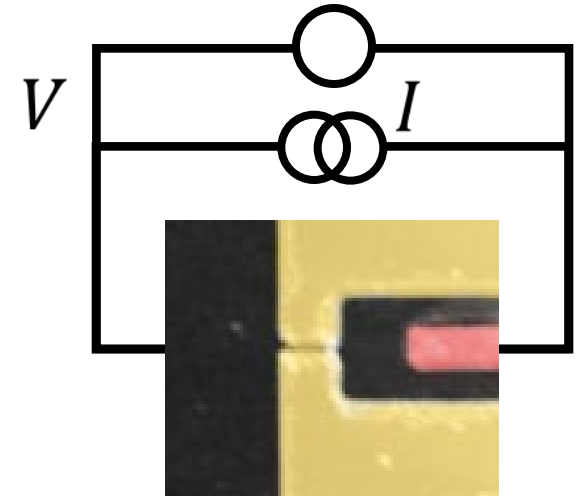
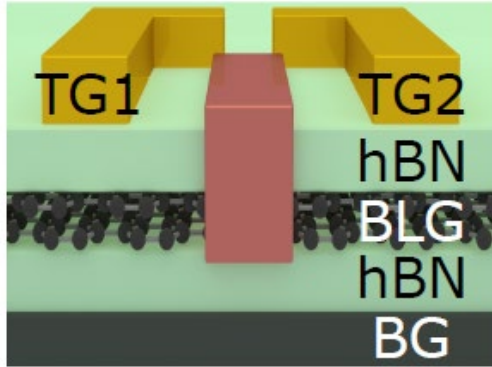
C. T. Foxon

*Philips Research Laboratories, Redhill, Surrey RH1 5HA, United Kingdom*

(Received 31 December 1987)

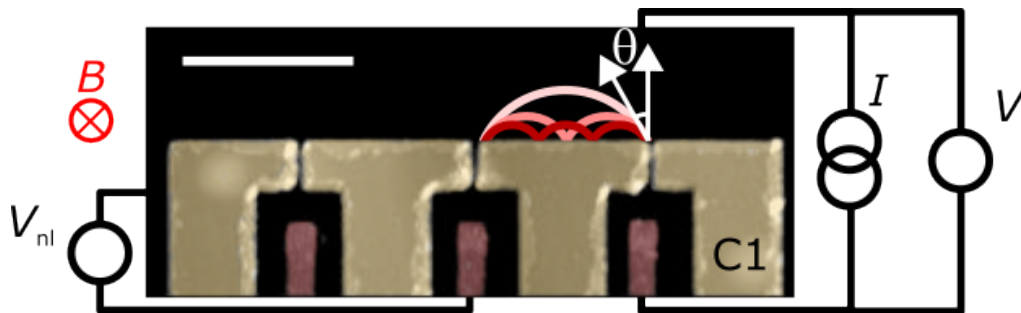
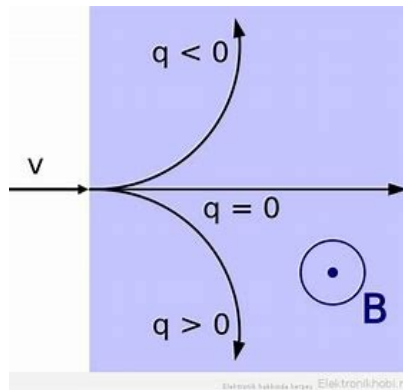


# basic characterization: band gap and quantum point contacts

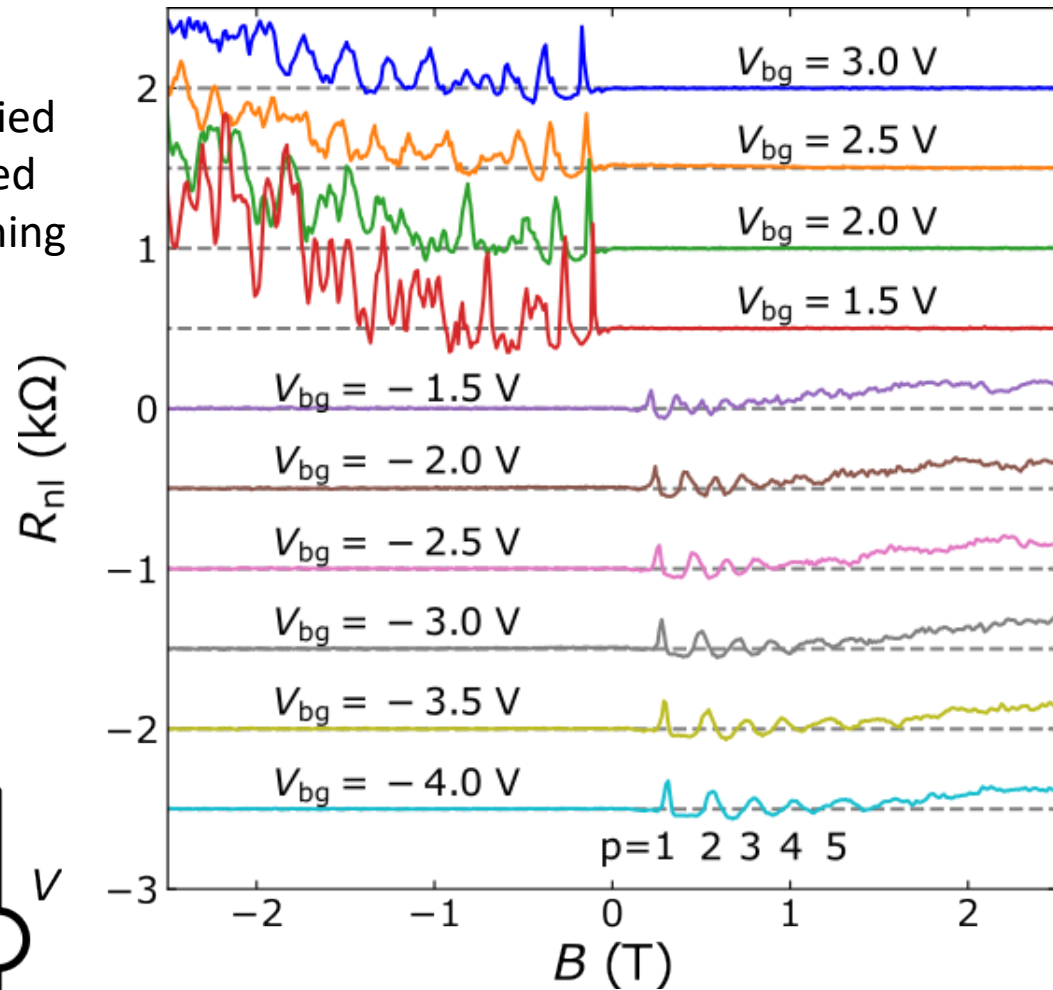


# transverse electron focusing BLG

- clear peaks observed indicating focussing
- electron side gives peaks for negative applied magnetic field and holes for positive applied fields, as expected (Lorentz force; has nothing to do with valleys)

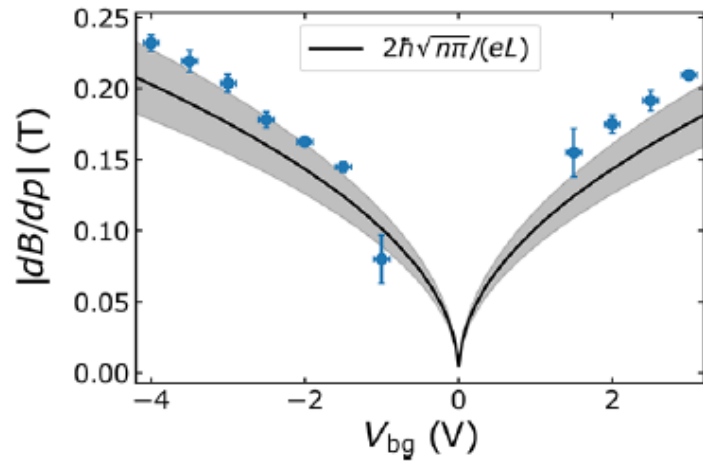


$$R_{nl} = V_{nl}/I$$



$T = 1.8$  K

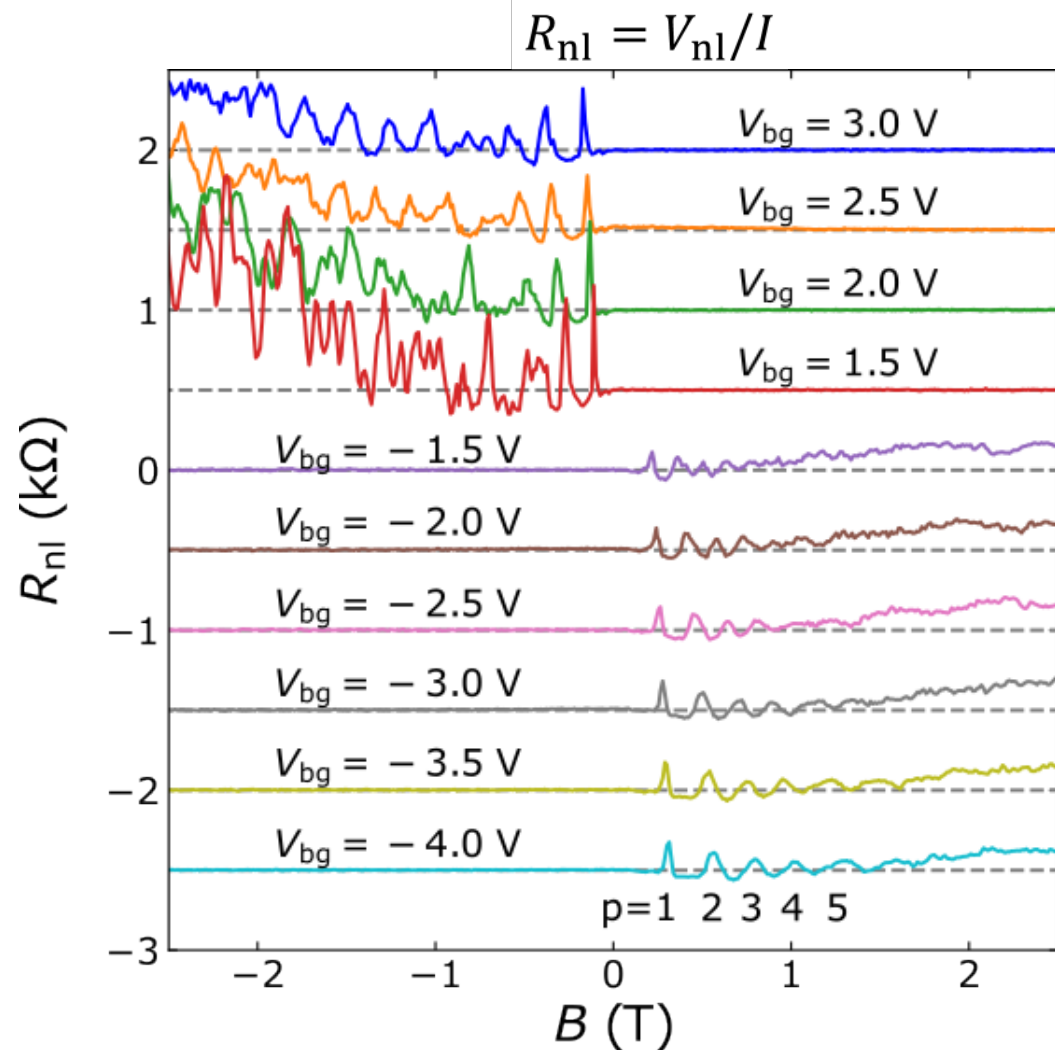
# transverse electron focusing: peak spacing increases with gate voltage



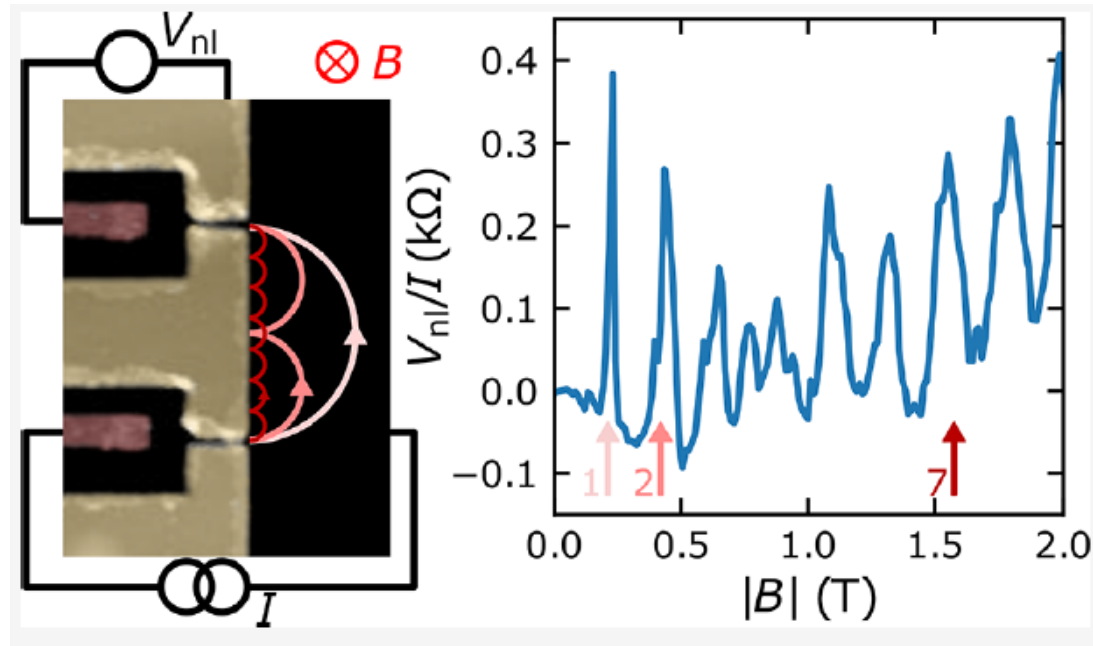
$$B_p = p^* (2mv_F / eL) \quad (p = \text{integer})$$

$$\text{peak spacing: } dB/dp = 2mv_F / eL$$

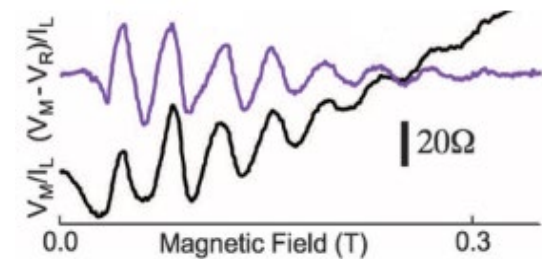
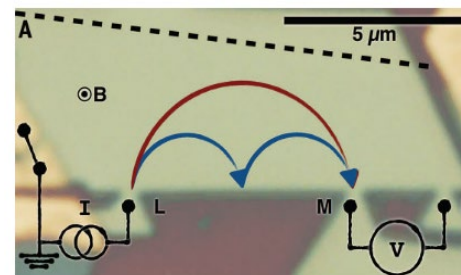
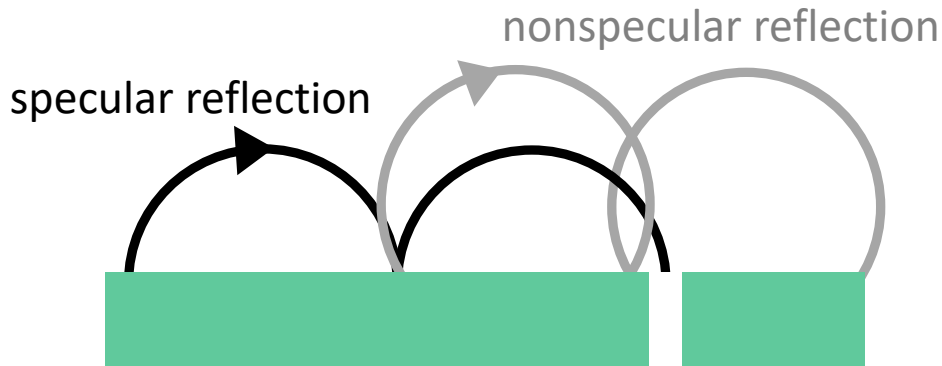
$$mv_F = \hbar k_F = \hbar(n\pi)^{1/2}$$



# transverse electron focusing: specular reflection

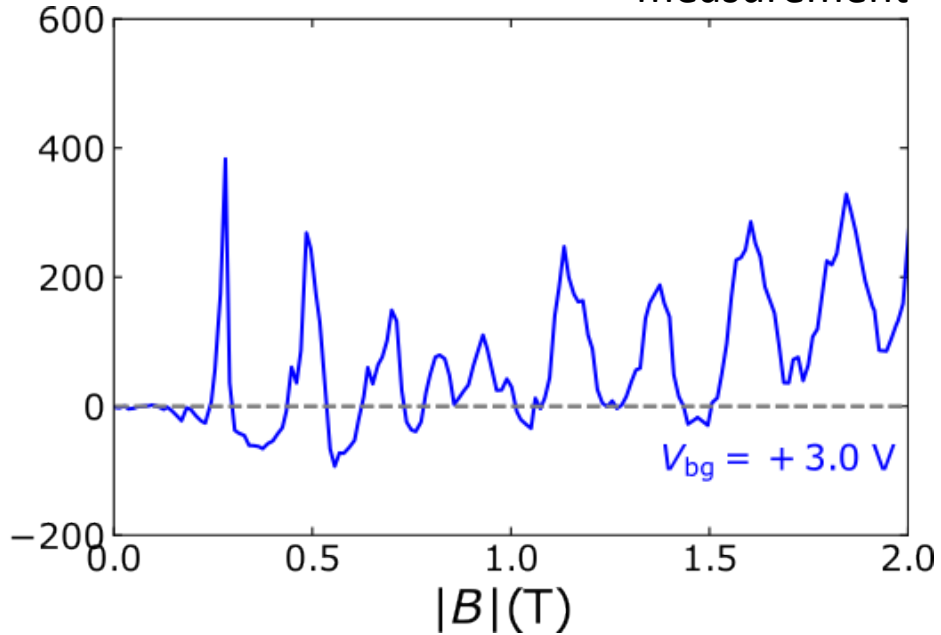


- previous work: only a few peaks observed due to incomplete specular reflection (graphene edges defined by etching)
- our work: electrostatically defined edges lead to the observation of many more peaks (specular reflection)

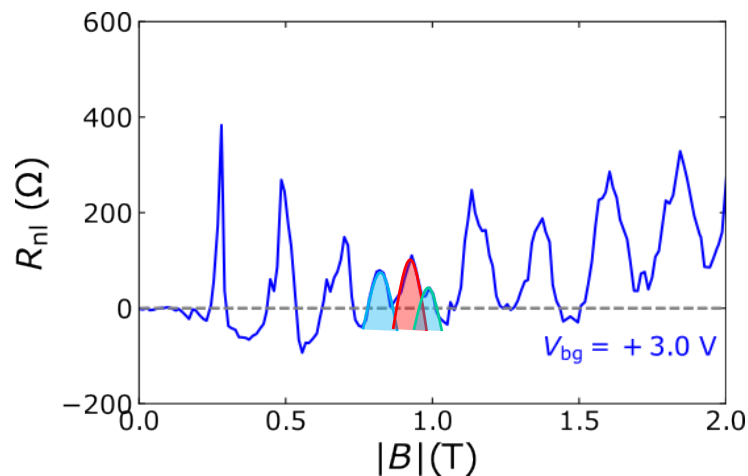
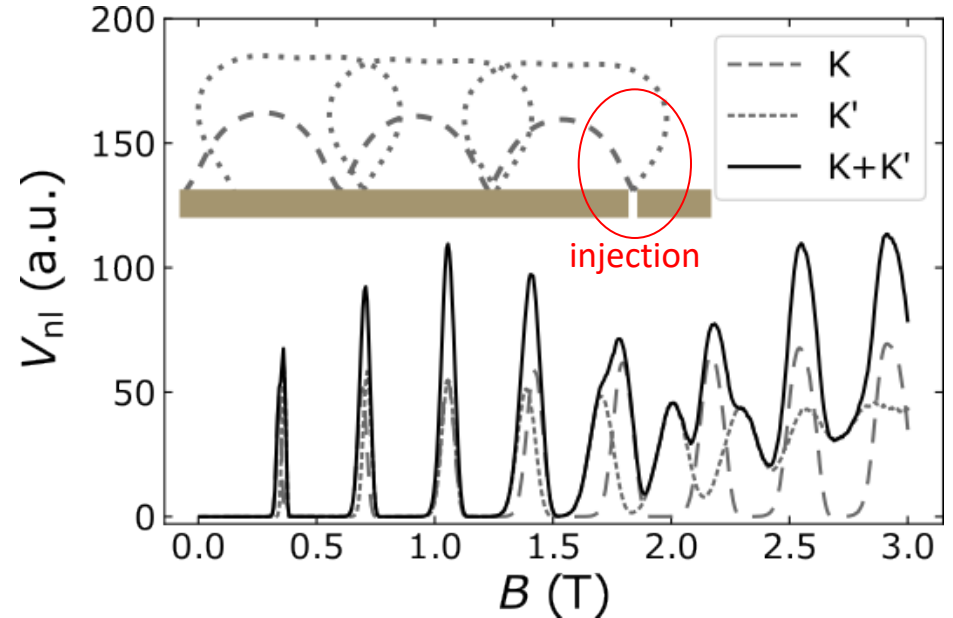


# transverse electron focusing: signatures of triangular warping

measurement



calculation

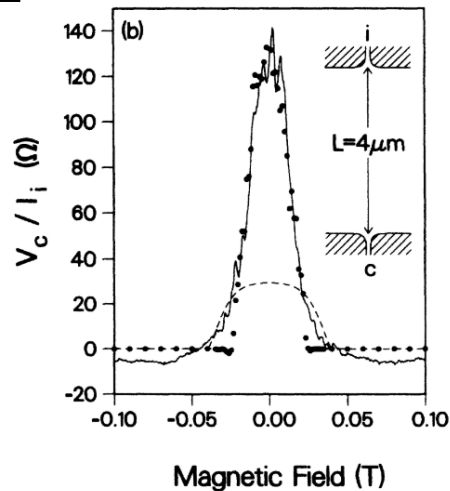
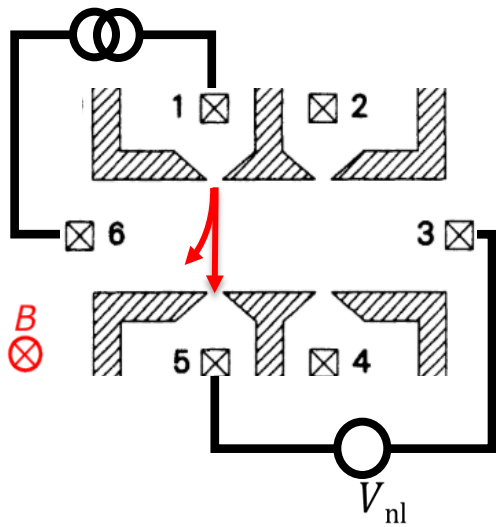


Valley selective focusing?

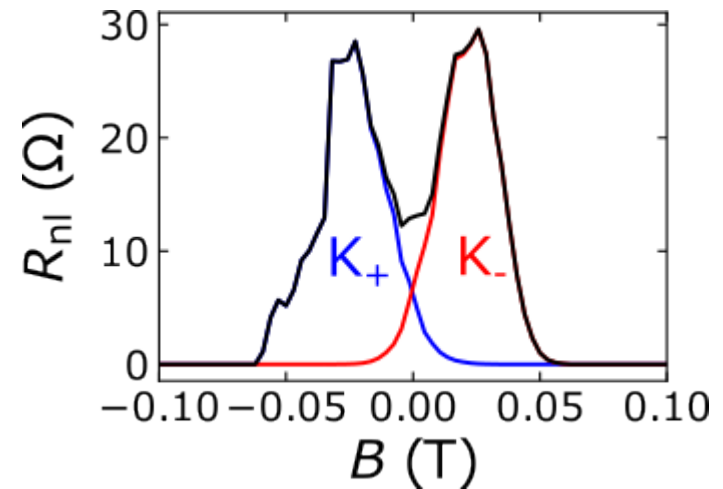
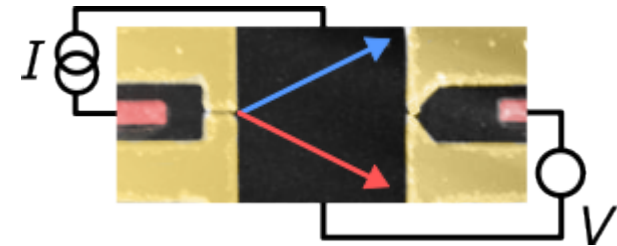
No definite proof because certain impurity configurations could in principle lead to similar behavior (unlikely though).

# collimation experiments with electron jets in ballistic BLG samples

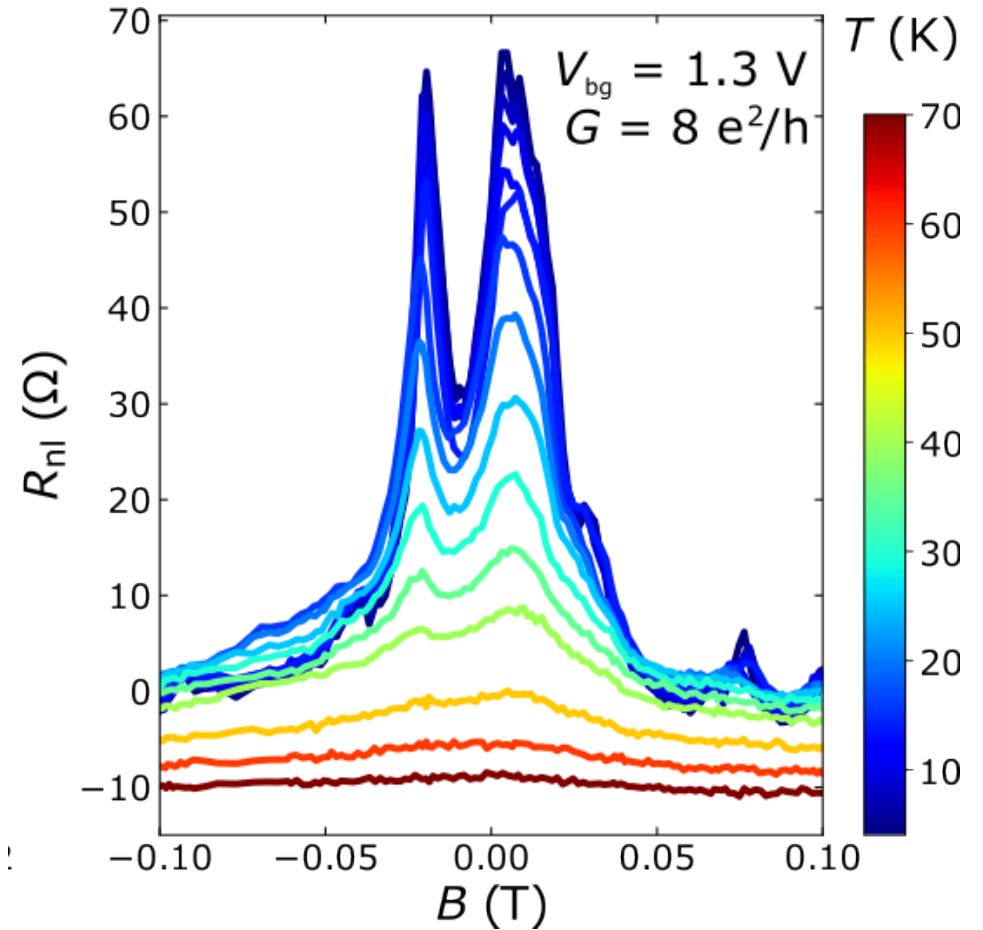
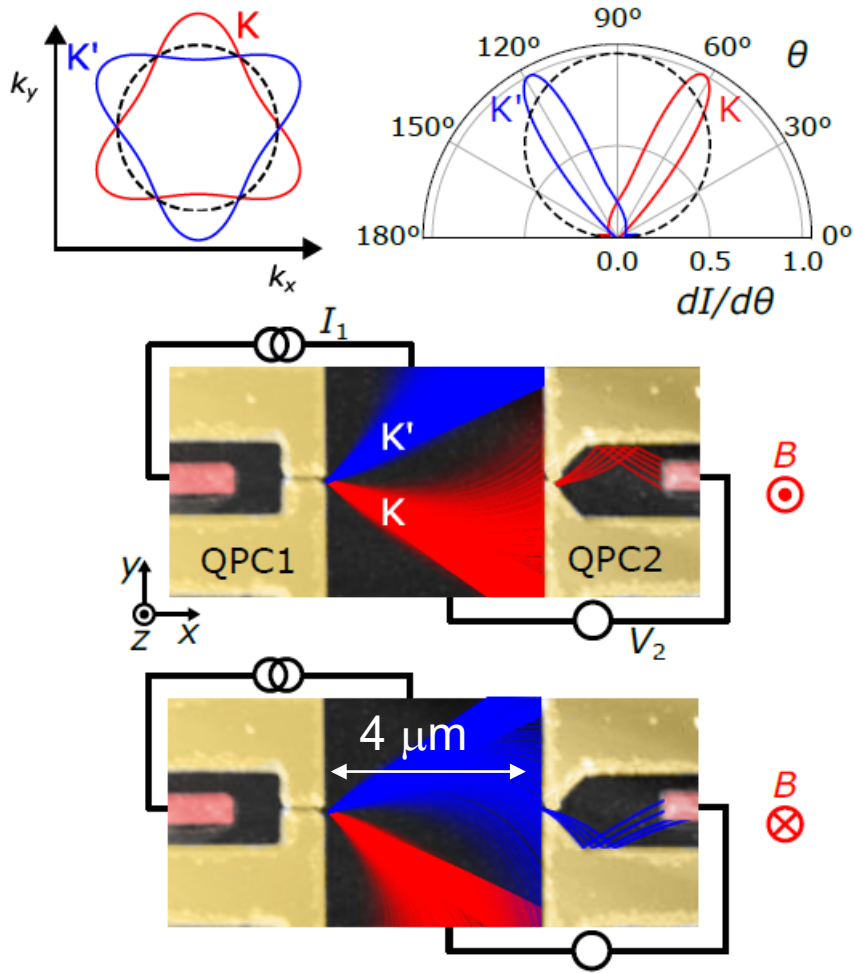
spherical Fermi surface: electron jet in one direction



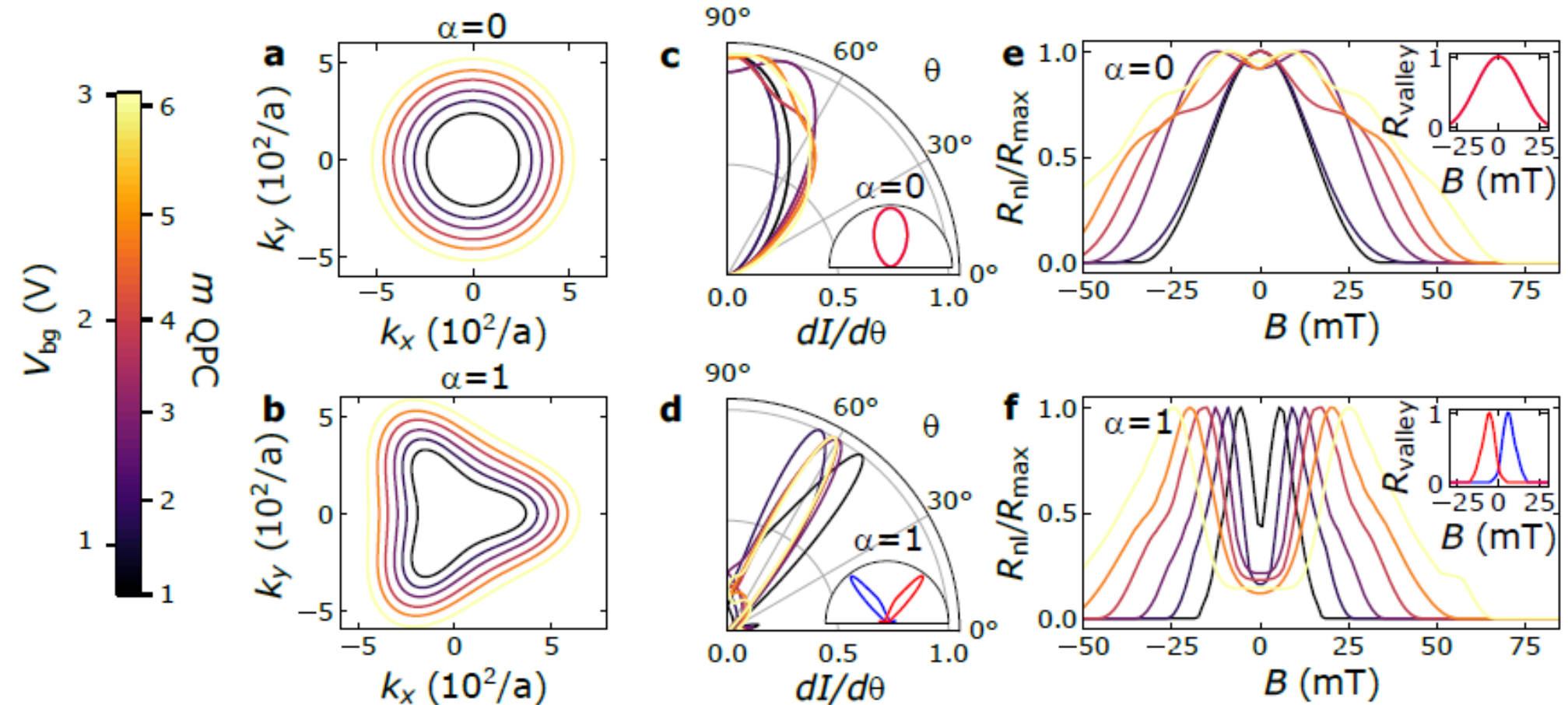
Fermi surface BLG: valley polarized jets in different directions



# collimation experiments in ballistic BLG samples

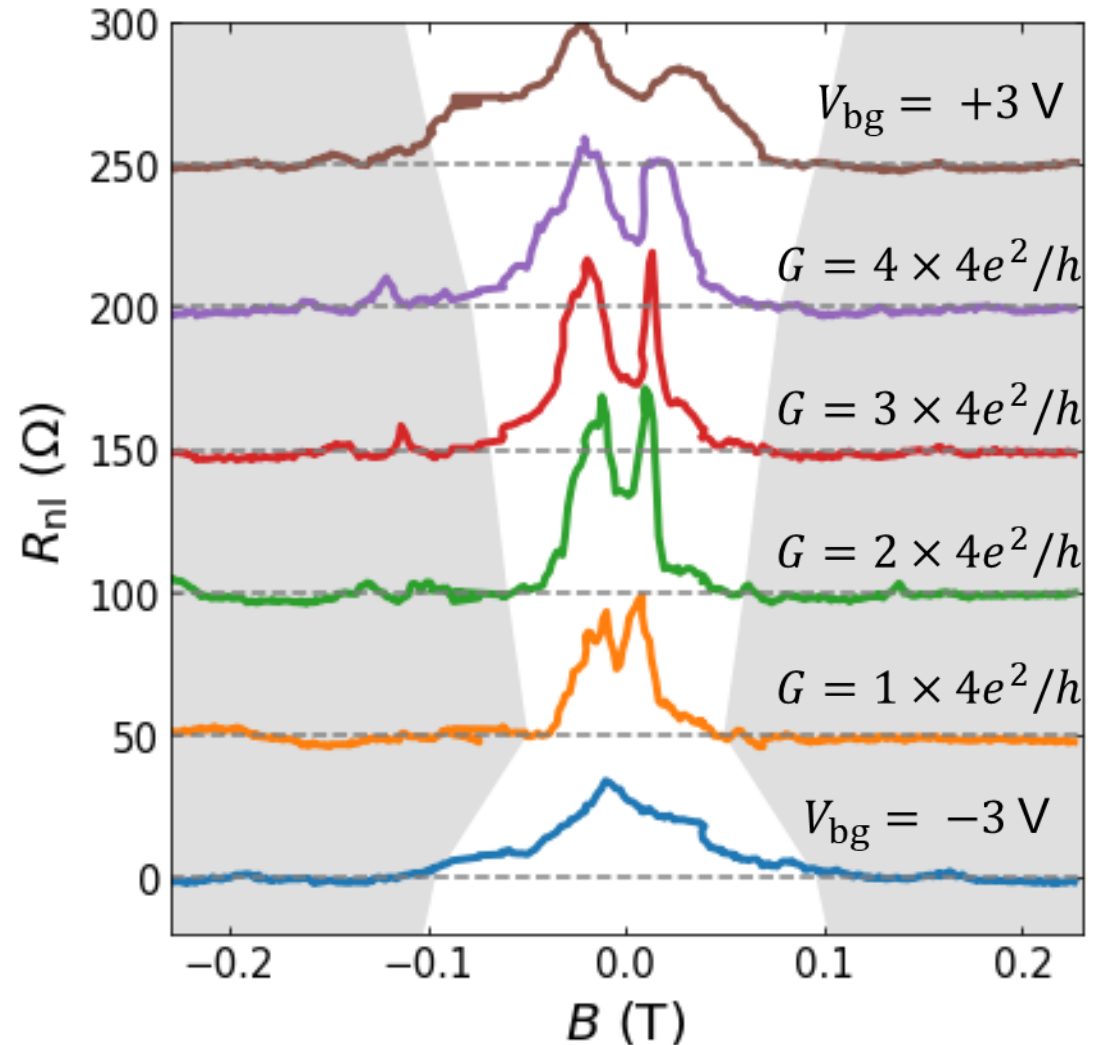
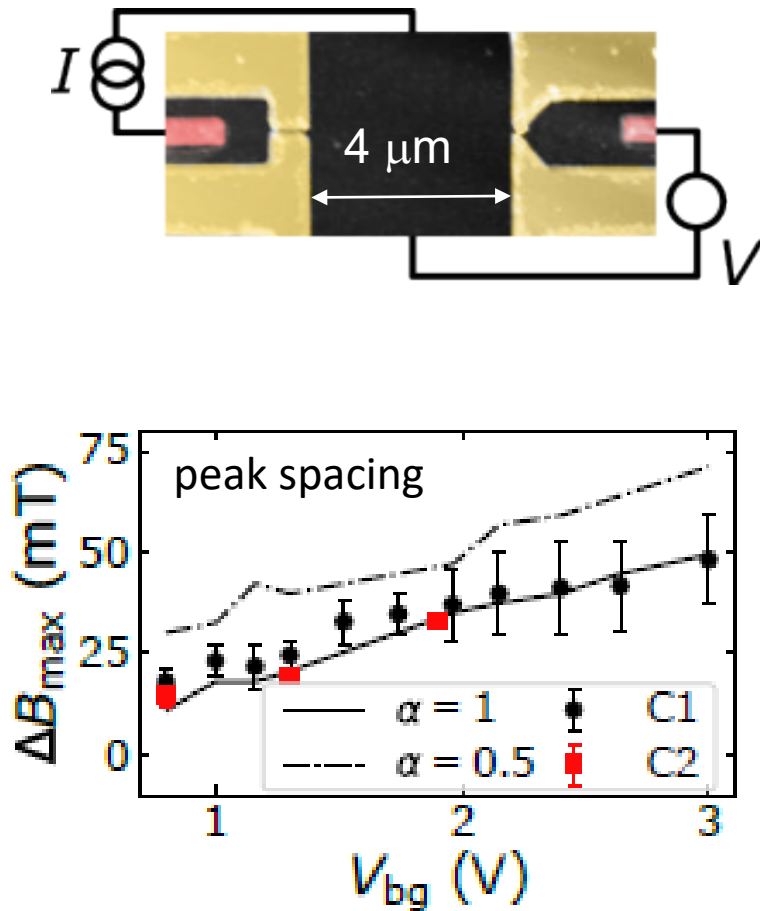


# semi-classical simulations for different back gate voltages



the peak spacing in the case of trigonal warping increases with doping (increasing back gate voltages)

# collimation experiments for different gate voltages

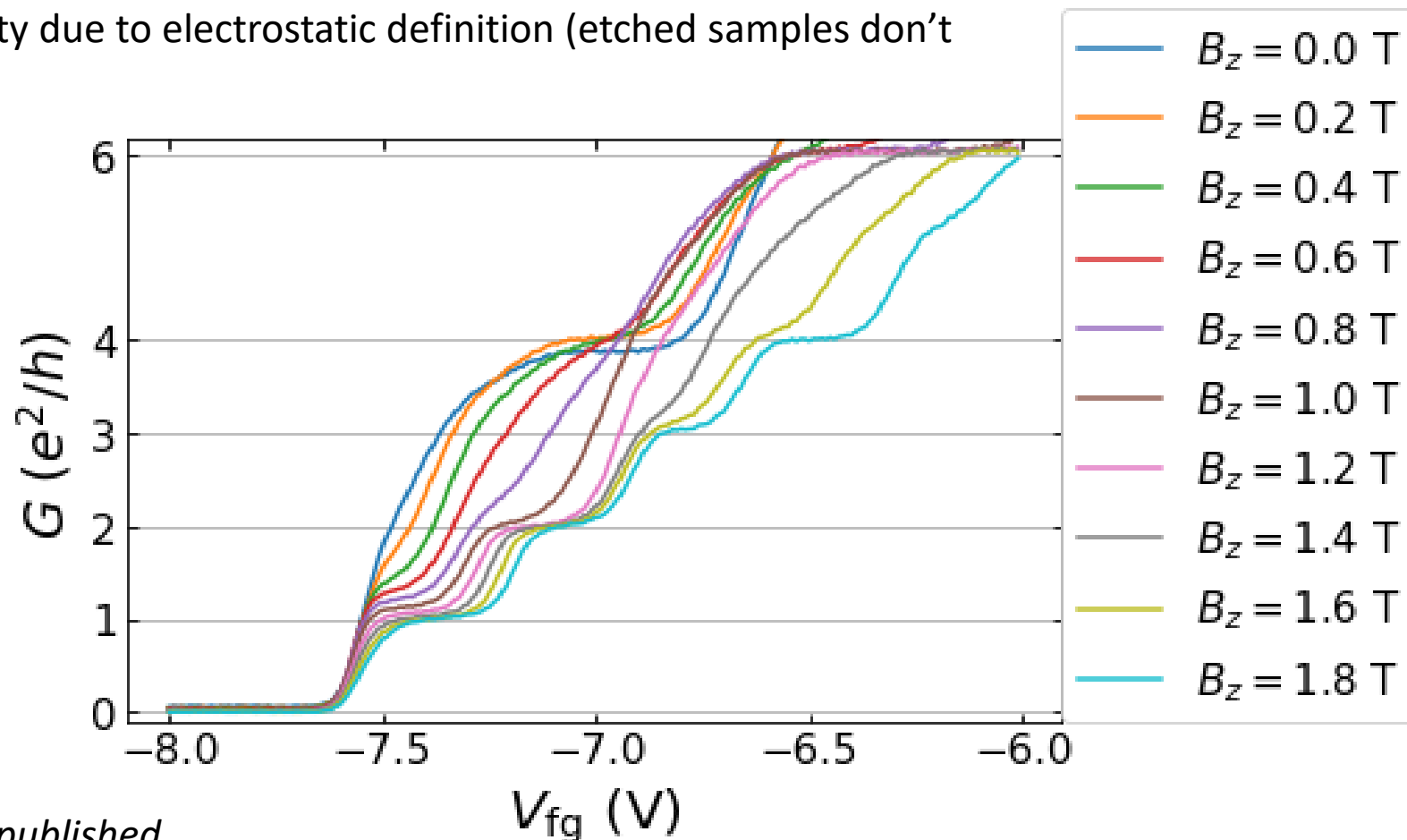


good agreement between semi-classical model and experiments indicating full trigonal warping ( $\alpha = 1$ ); visible only at the electron side where focusing works well

# Can we create spin-valley polarized currents?

quantum point contact (ballistic one-dimensional channel)

- quantized conductance steps ( $e^2/h$ )
- perpendicular magnetic field lifts both valley and spin degeneracy ( $B > 1.5$  T)
- high sample quality due to electrostatic definition (etched samples don't show this)



# quantum spin Hall states in graphene

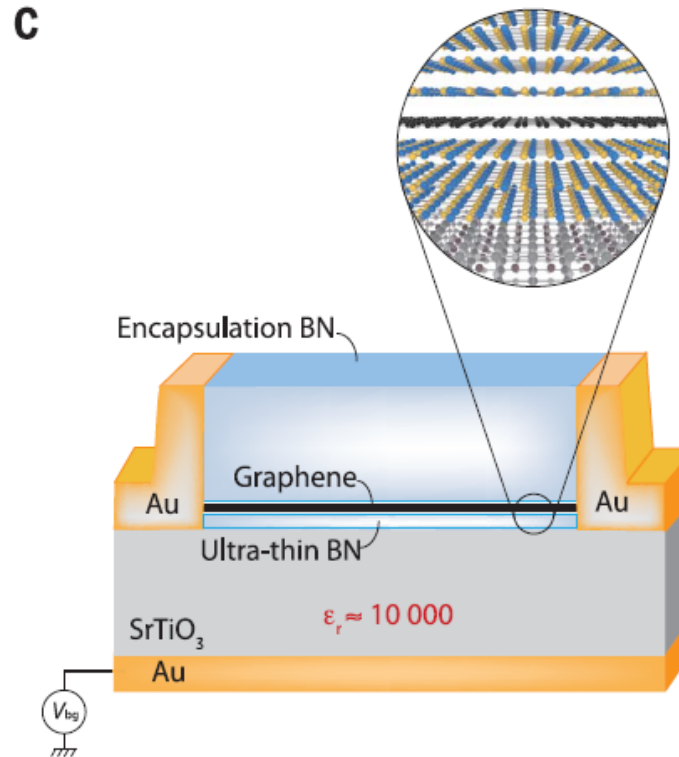
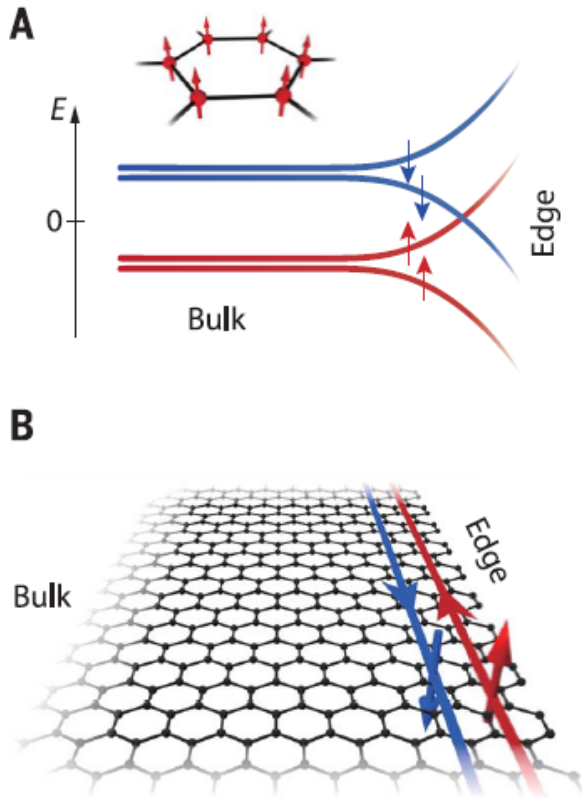
# quantum spintronics at zero (low) magnetic field

TOPOLOGICAL MATTER

Veyrat *et al.*, *Science* **367**, 781–786 (2020)

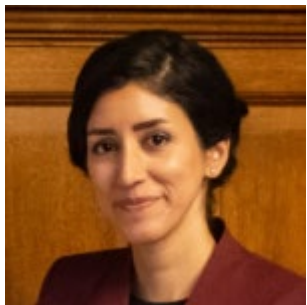
## Helical quantum Hall phase in graphene on SrTiO<sub>3</sub>

Louis Veyrat<sup>1</sup>, Corentin Déprez<sup>1</sup>, Alexis Coissard<sup>1</sup>, Xiaoxi Li<sup>2,3,4</sup>, Frédéric Gay<sup>1</sup>, Kenji Watanabe<sup>5</sup>, Takashi Taniguchi<sup>5</sup>, Zheng Han<sup>2,3,4</sup>, Benjamin A. Piot<sup>6</sup>, Hermann Sellier<sup>1</sup>, Benjamin Sacépé<sup>1\*</sup>



- quantum Hall topological insulator due to suitable screening of the Coulomb interaction with the high dielectric constant of the substrate
- helical edge states that are spin and valley filtered observed for magnetic fields as low as 1 T

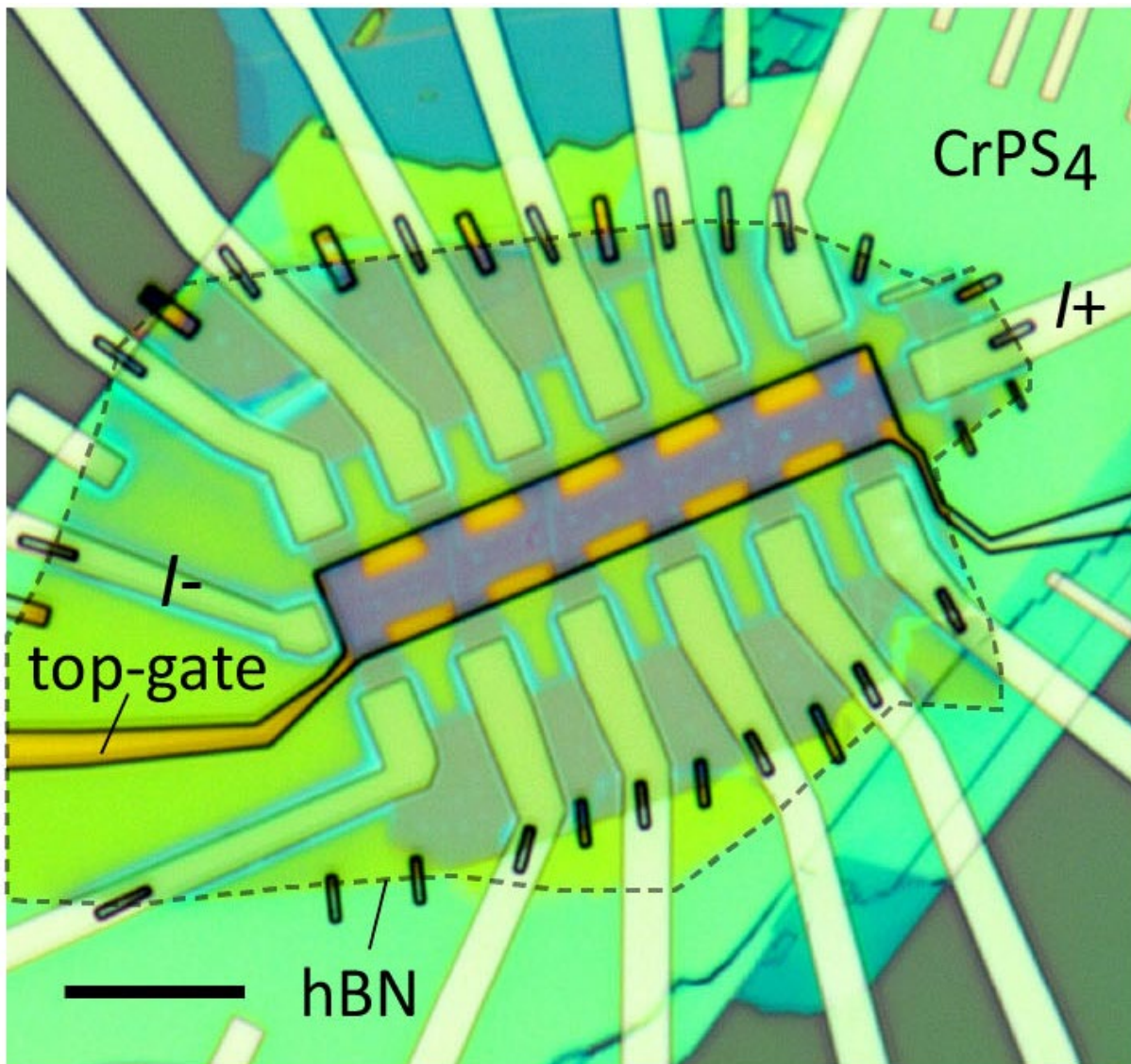
# induce magnetism in graphene Hall bar by the proximity of a 2D magnet



Talieh Giashi

combine the best of two materials:

- conducting graphene: long spin diffusion length
- insulating CrPS<sub>4</sub> (from Eugenio Coronado group): magnetism and introduces the broken inversion symmetry

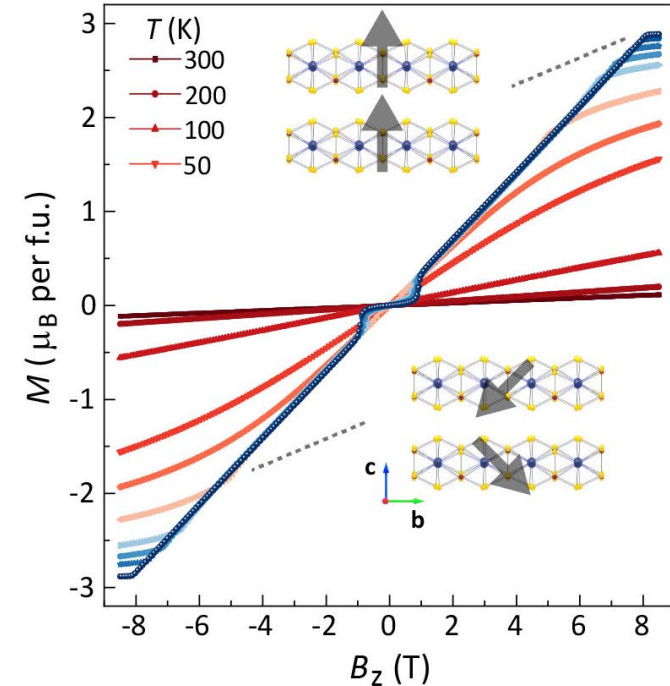
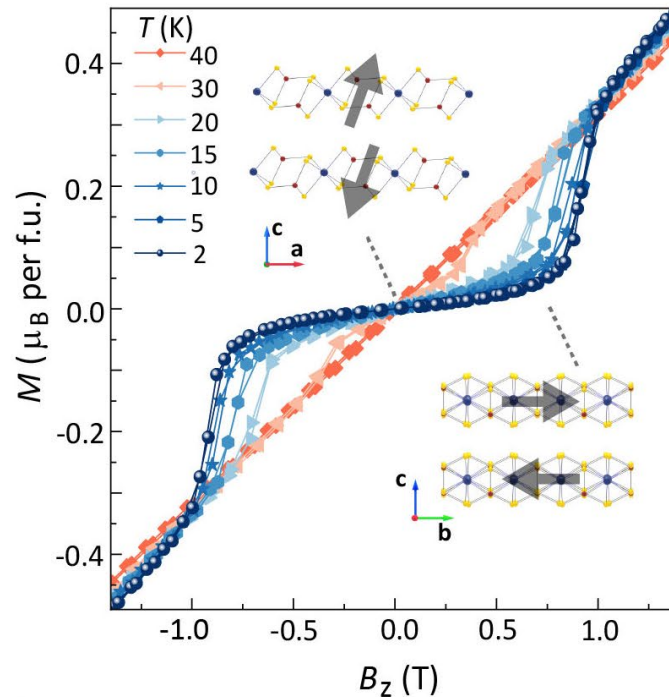
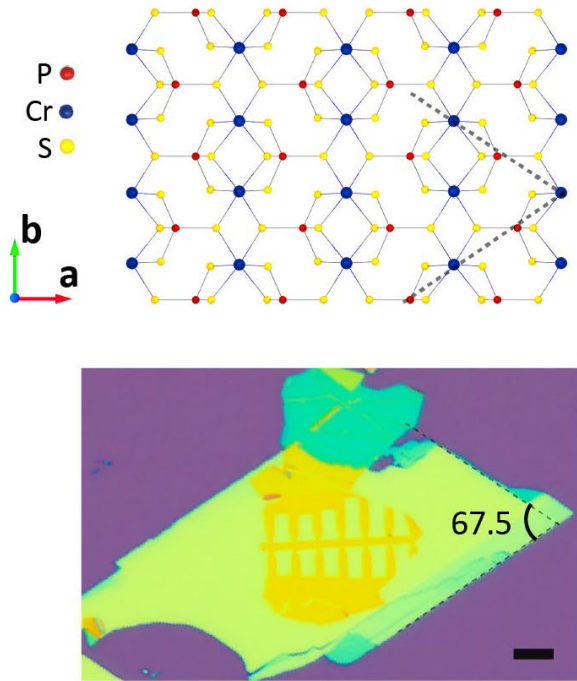


# the van der Waals 2D magnet CrPS<sub>4</sub>



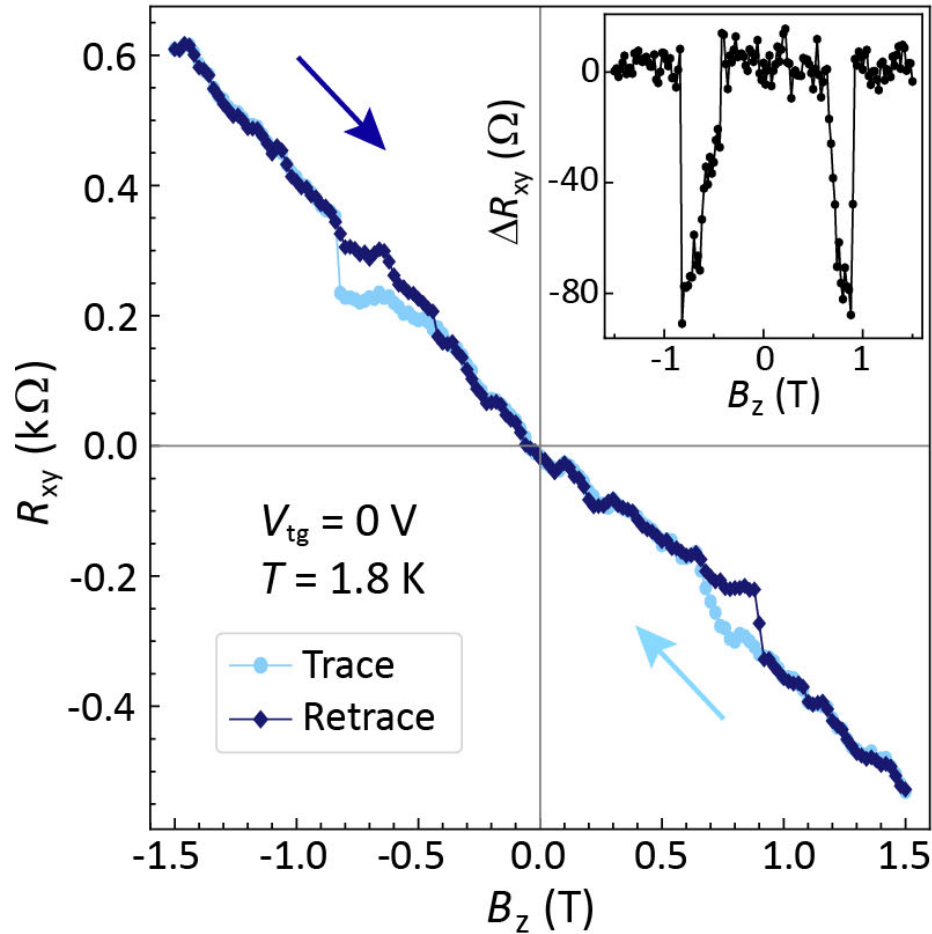
Samuel Mañas Valero

- interlayer antiferromagnet; more or less air-stable semiconductor with a bandgap of  $\sim 1.3$  eV and a Néel temperature of 38 K
- increasing  $B_z$  above the spin-flop transition field ( $B_{sf} \sim 0.8$  T at 2 K) results in canting of the magnetic moments towards the  $c$ -axis with full saturation at  $B_z = 8$  T

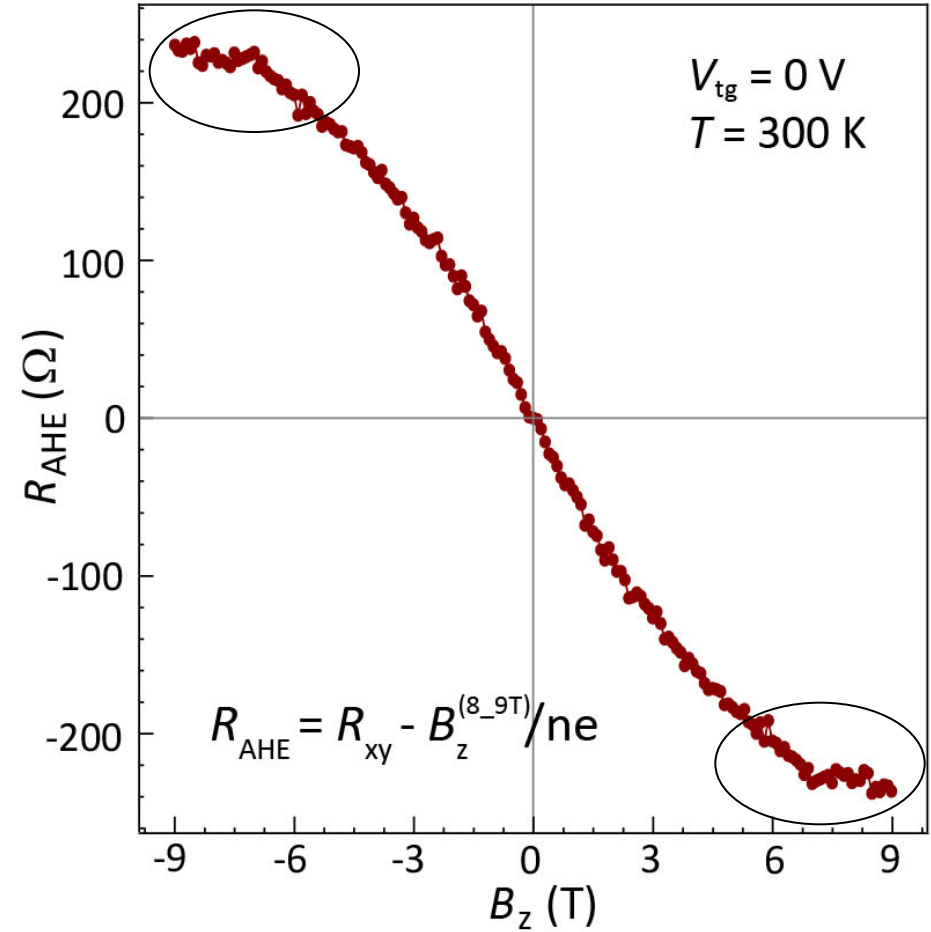


# signatures of magnetized graphene

hysteresis near the spin-flop transition

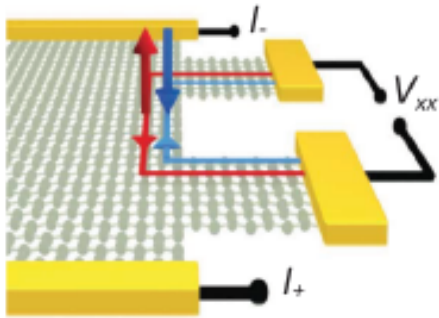


anomalous Hall effect: saturation of the Hall resistance at the saturation field

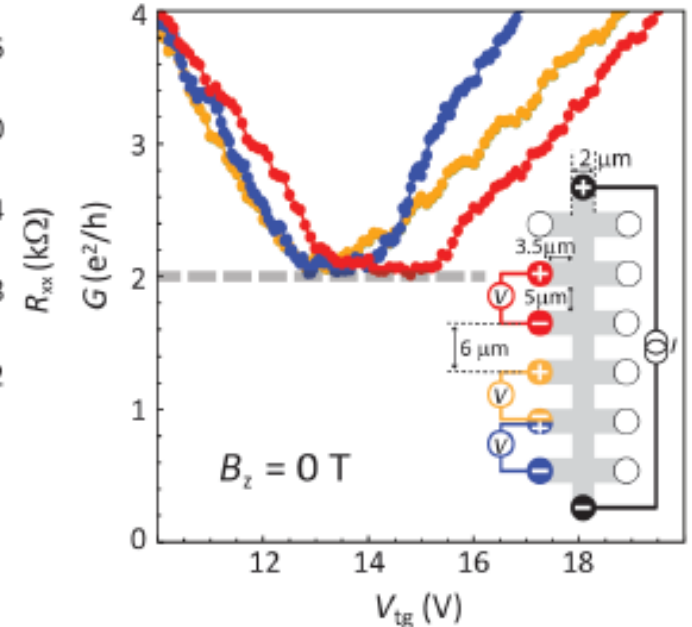
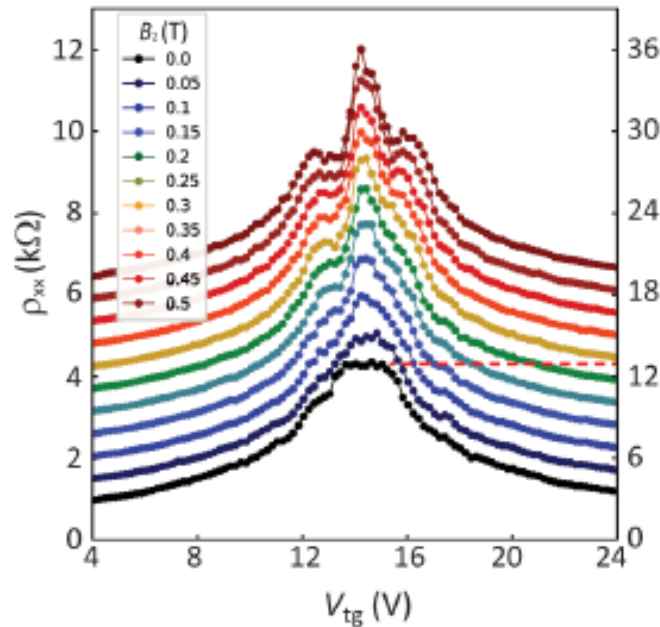


The observation of a sizable signal of 200  $\Omega$  is a signature of the co-presence of **large induced spin-orbit and exchange interactions** in the proximitized graphene up to room temperature

# quantum spin Hall states near zero magnetic field

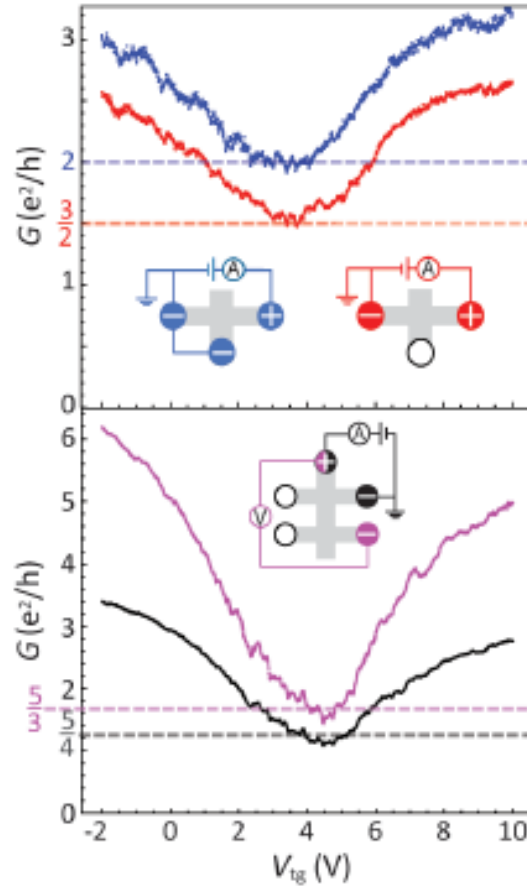
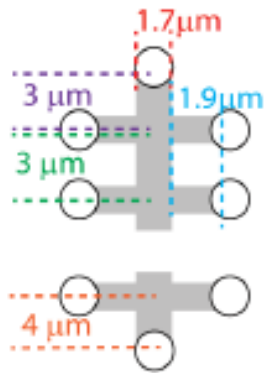


helical states are spin-polarized electron- and hole-like bands that counter propagate at the edges of the magnetized graphene



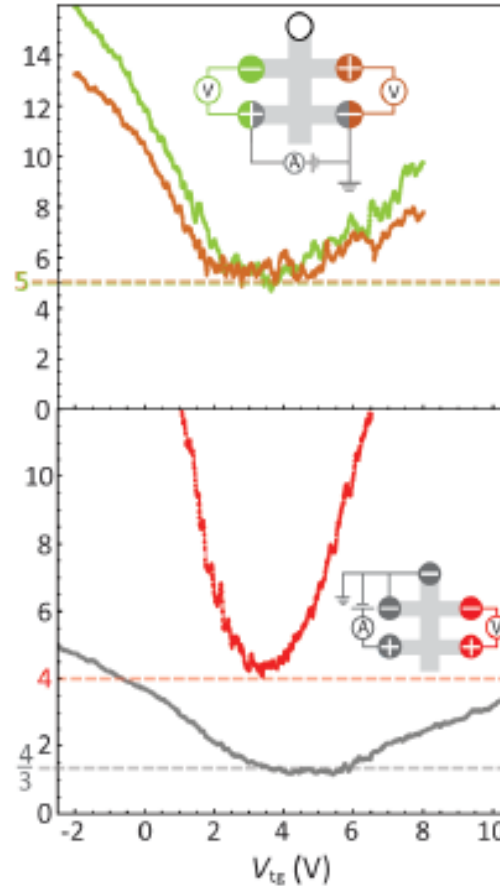
broadened resistance peak (conductance dip at  $2e^2/h$ ) is a sign for the existence of two edge states measured for different voltage pairs

# quantum spin Hall states at zero magnetic field



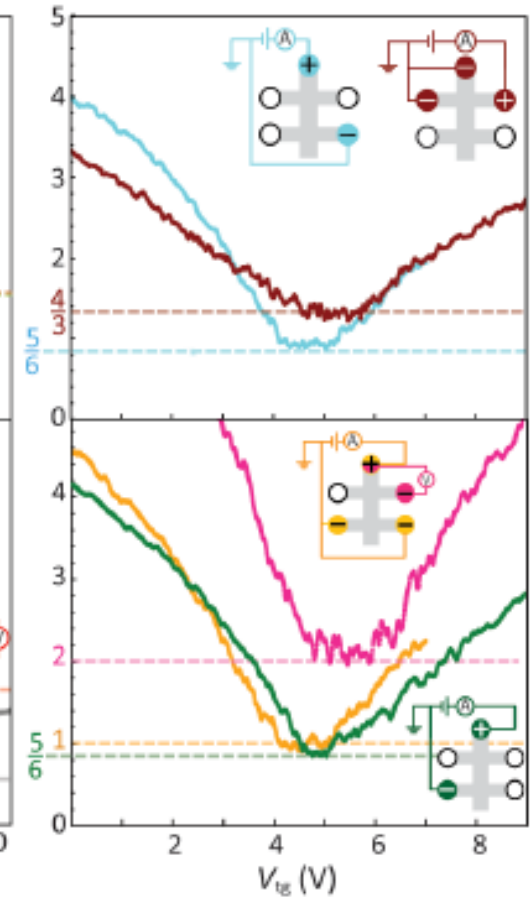
$$G_{2T} = \frac{e^2}{h} \left( \frac{1}{N_L + 1} + \frac{1}{N_R + 1} \right)$$

$N_{L,R}$ : number of floating probes along left/right edges



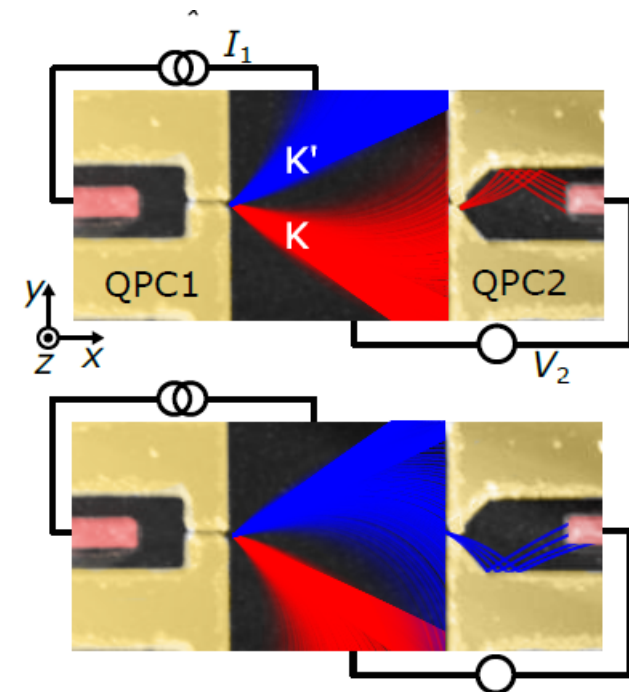
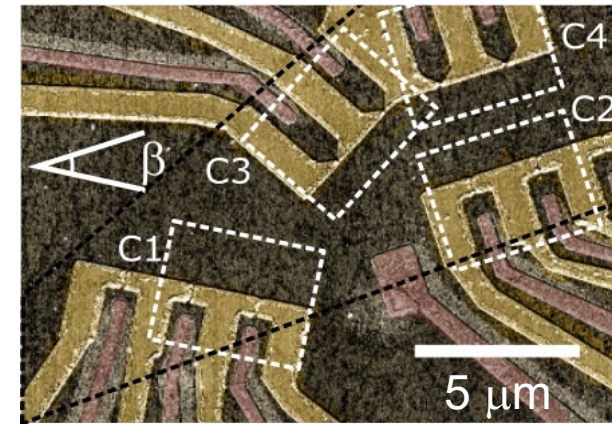
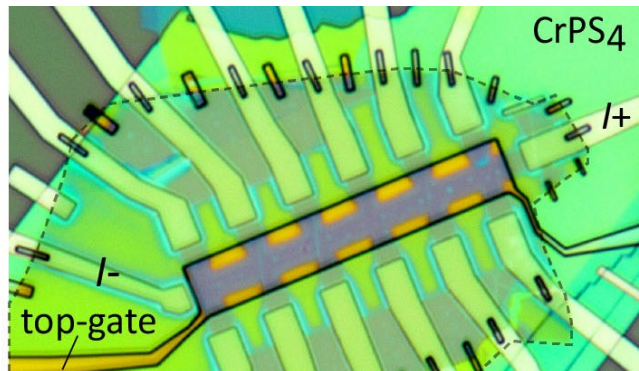
$$G_{4T} = G_{2T} \frac{N_I + 1}{N_V + 1}$$

$N_I$ : number of floating probes along edge where voltage is measured  
 $N_V$ : number of probes between voltage probes



# conclusion

- in 2D materials electrons, their spin and their presence in specific valleys can be used for quantum devices using different technology platforms
- broken inversion symmetry needed to access the valleys; bilayer graphene: use perpendicular electric field
- with electron focussing experiments valley polarized electron jets have been demonstrated in BLG
- next step: combine the different components into more complex devices



heterostructures of 2D materials offer many possibilities to fabricate new quantum devices